Universidade de Aveiro Departamento de Química
Ano 2014/2015

Pedro Flores Martins

Produção de extratos ricos em estigmasterol por extração supercrítica a partir de biomassa

Production of stigmasterol enriched extracts by supercritical fluid extraction of vegetable biomass

Universidade de Aveiro Departamento de Química
Ano 2014/2015

Pedro Flores Martins

Produção de extratos ricos em estigmasterol por extração supercrítica a partir de biomassa

Production of stigmasterol enriched extracts by supercritical fluid extraction of vegetable biomass

Tese apresentada à Universidade de Aveiro para cumprimento dos requisitos necessários à obtenção do grau de Mestre em Engenharia Química realizada sob a orientação científica do Doutor Carlos Manuel Silva, Professor auxiliar do Departamento de Química da Universidade de Aveiro, e sob a orientação do Engenheiro Marcelo Morais Melo, doutorando do Departamento de Química da Universidade de Aveiro.

o júri

presidente

Maria Inês Purcell de Portugal Branco

Professor auxiliar do Departamento de Química da Universidade de Aveiro

Carlos Manuel Santos da Silva

Professor auxiliar do Departamento de Química da Universidade de Aveiro

João Manuel do Paço Quesado Delgado

Investigador Auxiliar do CEC – Centro de Estudos das Construções da Faculdade de Engenharia da Universidade do Porto

agradecimentos

Apesar do caráter individual desta dissertação, todo o trabalho concretizado durante este período apenas foi possível devido ao apoio incondicional de várias pessoas às quais gostaria de expressar o meu mais honesto agradecimento:

em primeiro lugar, ao professor Carlos Silva pela amizade manifestada e pelos ensinamentos prestados ao longo do curso, pela disponibilidade e boa vontade em ajudar sempre que solicitado, e acima de tudo pela oportunidade concedida de trabalhar com um grupo de investigação tão fascinante;

ao amigo e coorientador Marcelo Melo, por todo o apoio prestado, pela grande amizade manifestada e por toda a instrução e valores transmitidos ao longo deste ultimo ano, um muito obrigado!

a todos os elementos do grupo de investigação EgiChem (Bruno Figueiredo, Simão Cardoso, Ana Magalhães, José Pedro, Andreia Silva), pelo apoio prestado, pela integração e por todos os momentos passados em boa companhia;

a todos os colegas e amigos de Engenharia Química, por fazerem parte de todo o meu percurso académico;

aos meus pais e irmão, por todo o apoio incondicional prestado em toda a minha vida.

Kinetics is nature's way of preventing everything from happening all at once.

- S. E. LeBlanc

palavras-chave Análise económica, *Eichhornia crassipes*, esteróis, extração supercrítica, modelação, *Moringa oleifera*

resumo

Neste trabalho, abordou-se a produção de extratos ricos em estigmasterol a partir de duas matérias-primas distintas por via da tecnologia de extração supercrítica, tendo como foco a otimização experimental de processo quer pela perspetiva técnica como pela económica

Relativamente à espécie *E. crassipes*, realizou-se um estudo de otimização das condições de operação com o objetivo de encontrar a melhor combinação de pressão e quantidade de co-solvente (etanol) que maximizasse o rendimento total, rendimento de esteróis e ainda a concentração de total e individual de esteróis no extrato final. Na gama de condições estudadas (200-300 bar e 0.0-5.0% (wt.) de etanol), as condições ótimas foram obtidas para 300 bar e 5.0% de etanol, obtendo-se 1.24% de rendimento total; e 300 bar e 2.5% de etanol quer para o rendimento como para a concentração de esteróis. De modo a estudar o passo limitante no transporte de massa do processo, 4 curvas de extração foram medidas para diferentes caudais e % de co-solvente, e diferentes modelos fenomenológicos simplificados foram ajustados aos dados experimentais, tendo-se observado que os modelos baseados nas hipóteses de controlo por difusão proporcionam um melhor ajuste.

Relativamente à espécie *Moringa oleifera*, um estudo tecno-económico abrangendo a coprodução de óleo e de esteróis foi realizado usando a abordagem de optimização (RSM) de custo de produção (COM) que incluiu o custo de secagem inicial da matéria-prima, separação final dos esteróis do óleo, para além dos custos diretamente associados ao processo de extração supercrítica. Nas condições ótimas de pressão e tempo de extração de 350 bar e 1.3h, respetivamente, $COM_{óleo}$= 2.64 $€\,kg_{óleo}^{-1}$ para uma unidade de extração composta por dois extratores de $1m^3$ cada. No caso da coprodução de uma mistura de esteróis com 89.4 wt.% de pureza, o $COM_{esteróis}$ mínimo é de 5.11 $€\,kg_{esteróis}^{-1}$. Nestas condições a produção anual ascende a 558.9 $ton_{óleo}$ e 1.9 $ton_{esteróis}$. No processo estudado, estima-se um lucro de 15.94 $M€\,ano^{-1}$, mostrando que o processo integrado proposto é viável e que existem sinergias económicasque não deverão ser negligenciadas.

De um modo geral, este trabalho abre caminhos de exploração destas duas matérias-primas por via da extração supercrítica, no âmbito do conceito de biorefinaria.

keywords *Eichhornia crassipes,* economic analysis*,* modeling*, Moringa oleifera,* sterols, supercritical fluid extraction

abstract The production of stigmasterol enriched extracts from two different vegetal raw materials, *Eichhornia crassipes and Moringa oleifera* was assessed in this work, targeting at process optimization and economic analysis through supercritical fluid extraction (SFE)

Regarding *E. crassipes*, the optimization of the operating conditions aimed at obtaining the best combination of pressure and ethanol content that maximizes total extraction yield, total sterols extraction yield and total and individual sterols concentration in the extract. In the range of operating conditions studied (200-300 bar and 0.0-5.0% (wt.) ethanol content),the optima were found for 300 bar and 5% ethanol for total extraction yield, amounting 1.24%; and 300 bar and 2.5% ethanol for both total sterol yield and total sterols concentration, . As to disclose the rate determining step of the extraction process, six extraction curves were measured for different flow rates and ethanol content, and three simplified phenomenological models were adjusted to the experimental data, with models based in diffusion controlled assumptions providing the best fitting adequacy.

For the SFE of *Moringa oleifera* seed oil, a techno-economic study encompassing the coproduction of oil and sterols was accomplished using the RSM-COM approach, where the costs of drying of the biomass and separating the sterols from the bulk oil were taken into account besides the supercritical fluid extraction expenses. For a SFE unit comprising two-extractors of 1 m^3 capacity and operating under optimum pressure and time conditions of 350 bar and 1.3 h, respectively, the cost of manufacturing (COM) of the oil was estimated to be 2.64€ $\mathrm{kg}_{\mathrm{oil}}^{-1}$. For the coproduction of a sterols mixture with 89.4 wt. % purity, the minimum $COM_{sterols}$= 5.11€ $\mathrm{kg}_{\mathrm{sterols}}^{-1}$. The overall annual production of oil and sterols under these conditions is 558.9 tons and 1.9 tons, respectively. The most favorable net income of the studied process reaches 15.94M€ year^{-1}, showing the proposed integrated process to be feasible, and that non negligible cost synergies exist.

In the whole, the study opens the way to exploit these raw materials by supercritical fluid extraction within the scope of biorefinery premises.

Table of Contents

List of Figures

List of Tables

Nomenclature

Symbol	Units	Name
a_0	$\mathrm{m}^2 \cdot \mathrm{m}^{-3}$	Specific external surface area
a_i		Chrastil equation parameters
BBD		Box-Behneken Design
CCD		Central Composite Design
CER		Constant Extraction Rate
COL	$€ \cdot \mathrm{year}^{-1}$	Cost of labor
COM	$€ \cdot \mathrm{year}^{-1}$	Cost of Manufacturing
CRM	$€ \cdot \mathrm{year}^{-1}$	Cost of Raw Material
CUT	$€ \cdot \mathrm{year}^{-1}$	Cost of Utilities
CWT	$€ \cdot \mathrm{year}^{-1}$	Cost of Waste Treatment
D_{12}	$\mathrm{cm}^2 \cdot \mathrm{s}^{-1}$	Diffusion Coefficient
DC		Diffusion Controlled
DM		Diffusion Model
DoE		Design of Experiments
EoS		Equation of State
EtOH		Ethanol
FER		Falling Extraction Rate
GC-MS		Gas Chromatography-Mass Spectrometry
H	$\mathrm{m}^3_\mathrm{solid} \cdot \mathrm{m}^{-3}_\mathrm{fluid}$	Partition coefficient/equilibrium parameter
ΔH	$\mathrm{J} \cdot \mathrm{mol}^{-1}$	Heat of reaction (vaporization plus solvation)
k_1		Association factor
k_d	h^{-1}	Desorption constant
k_film	$\mathrm{m} \cdot \mathrm{h}^{-1}$	Mass transfer film coefficient
L_b	m	Bed length
LEFM		Linear Equilibrium plus Film resistance Model
MeOH		Methanol
P	bar	Pressure
$\dot{\mathrm{Q}}$	$\mathrm{kg} \cdot \mathrm{h}^{-1}$	Mass flow rate
$\Re$	$\mathrm{J} \cdot \mathrm{mol}^{-1}\mathrm{K}^{-1}$	Universal gas constant
r	m	Particle radius
R^2		Coefficient of determination
RDS		Rate Determining Step

RSM		Response Surface Methodology
S	m^2	Extractor cross section
SC		Supercritical
SCF		Supercritical Fluid
SFE		Supercritical Fluid Extraction
SLE		Solid-Liquid Extraction
SSPM		Simples single plate model
T	℃	Temperature
t	s	time
u	$\mathrm{m} \cdot \mathrm{h}^{-1}$	Superficial velocity
w	kg	mass
$X_\mathrm{i}/x_\mathrm{i}$		Coded Variable/ True Variable
X_0	$\mathrm{kg}_{\mathrm{extract}} \cdot \mathrm{kg}_{\mathrm{biomass}}^{-1}$	Soxhlet extraction yield
y	$\mathrm{kg} \cdot \mathrm{m}^{-3}$	Solute concentration in the fluid phase
y_s	$\mathrm{kg} \cdot \mathrm{kg}_{\mathrm{biomass}}^{-1}$	Solute concentration in the biomass
y'	$\mathrm{kg}_{\mathrm{solute}} \cdot \mathrm{m}_{\mathrm{solid}}^{-3}$	Surface equilibrium concentration

Geek letter	**Unit**	**Name**
β_i		Regression model coefficients
ε	$\mathrm{m}_{\mathrm{fluid}}^3 \cdot \mathrm{m}_{\mathrm{bed}}^{-3}$	Porosity
δ	$\mathrm{bar}^{1/2}$	Hildebrand solubility parameter
η		Yield
μ	$\mathrm{g} \cdot \mathrm{cm}^{-1} \cdot \mathrm{s}^{-1}$	Dynamic viscosity
ν	$\mathrm{m}^2 \cdot \mathrm{s}^{-1}$	Kinematic viscosity
ρ	$\mathrm{g} \cdot \mathrm{cm}^{-3}$	Density
θ	m	Plate thickness

Subscript	**Name**
adj	adjusted
b	biomass
c	critical
eb	boiling point
f	fluid
s	solid
stigm	Stigmasterol

Scopes and aims of the present work

Over the past decade, environmental friendly processes have been increasingly reported in the literature with great emphasis in a broad field of areas, such as product and waste valorization, increase in process productivity and even sustainability assessments.

Supercritical technology is, at the moment, one of the most debated green technologies with a tremendous versatile applicability, being highlighted the extraction processes, purification, bio-fuels production, material processing and working fluids.

Supercritical fluid extraction (SFE) of vegetable biomass using CO_2 as extraction solvent has been widely discussed due to the great potential that this technology offers: the advantages that SFE provides in the extraction of bioactive components (for example selectivity, easy separation of the solvent from the extract, moderate extraction temperatures) causes realistic expectation in the future industrial implementation of this type of process [1–7]. At the present time, the most important markets for these natural extracts rely in applications focused in the food, nutraceutical, pharmaceutical and cosmetic industries. In the last years several SFE units have been installed in India, New Zealand, Spain, Denmark and other countries, to exploit biomass raw materials as different as herbs, spices, hops, rice, cork, etc [8].

In this context, this work has the aim of studying the SFE of *E. crassipes* and *M. oleifera*, for the obtainment of stigmasterol enriched extracts focusing in process optimization both at technical and economic perspectives. Also, it provides a pertinent contribution for the valorization of these two raw materials, whose extracts production imply quite distinct potential industrial volumes and concentrations regarding the target compounds. The systematized contribution of this work (1 article published, 1 article submitted and 1 article in preparation) regarding typical research stages in SFE processes are presented in Table 1, including its interlink with existing works from the literature.

The structure of the document is as follows: in Chapter 1 several introductory remarks regarding the vegetable species and their extractives, supercritical fluids, extraction processes and mathematical modeling are presented; in Chapter 2 the optimization of the SFE of *E. crassipes* is assessed; Chapter 3 consists in the techno economic study of the co-production of stigmasterol and oil from *Moringa oleifera* seed; in Chapter 4 the overall conclusions are displayed and finally; in Chapter 5 some suggestions for future work are given.

Table 1 – Sorted stages of study in SFE processes and references of works already developed in said stages

	Raw material Characterization	Preliminary SFE study	Optimization of the operating conditions	Extraction curves and modeling	Pilot studies	Economic analysis
E. crassipes	[9]	[14]	This work [16]*	This work [16]*	-	-
M. oleifera	[10]	[11]	[12]	[11]	[13]	This work [15]

*Article in preparation

1. Introduction

1.1. *Eichhornia crassipes* and *Moringa oleifera* – two promising sources of stigmasterol and other valuable sterols

Eichhornia crassipes, commonly known as water hyacinth, is an aquatic plant native from the Amazon basin in South America. This plant is mostly found in lakes, rivers and reservoirs due to the high content of nutrients in this areas. Being considered an invasive plant, one of its main characteristics is the high growth rate, as it can reach up 17.5 tons per hectare per day if in favorable conditions [17]. Outside its original ecosystem, and as a consequence of exhibiting a weed type of behavior, this plant has been considered one of the most problematic worldwide, causing a reduction of fishing sites area, interfering with hydroelectric energy production sites, among other problems [18].

Despite the problematic infesting behavior, *E. crassipes* can be used as a useful resource in a wide field of applications. In the XXI century, this plant has been considered as a green alternative source to fossil fuels, since it allows the production of biogas at low cost and presents low atmospheric emissions [17,19]. In addition, water hyacinth is also used as a biologic fertilizer and as a biosorbent for treatment of waste waters, since its roots can naturally absorb toxic components and heavy metals [17].

Regarding the chemical composition of *E. crassipes*, the water content present in this plant can attain values as high as 95% of its weight. Moreover, organic matter comprises only 3.5% of the raw weight, being able to reach a fraction higher than 75% when in a dry basis [17]. In terms of extractives, a recent study evidenced that *E. crassipes* contain several sterols, namely stigmasterol, β-sitosterol and campesterol (methylcholesterol) [9,20], whose structures are illustrated in Figure 1. As a result, a potential valorization strategy for water hyacinth may encompass its exploitation as a source of sterols (namely stigmasterol), which are highly sought in view of their medicinal properties [21].

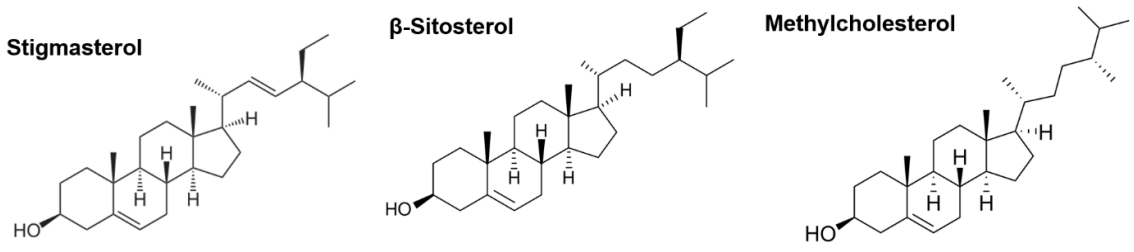

Figure 1- Chemical structures of the main phytosterols present in the extract of *E. crassipes*

Moringa oleifera seeds extracts are also a source of sterol mixture comprising β-sitosterol, stigmasterol, campesterol and Δ^5-avenasterol. This plant is original from northwestern India but commonly found in many tropical areas, and due to the high nutritive value, various parts of this plant are used as edible items in many locations [22,23]. *M. oleifera* oil, also known as ben oil, is the main product obtained when submitting moringa seeds to an extraction process. This oil consists in up to 40% of the plant seed weight, and its composition comprise high contents of oleic acid, behenic, palmitic and stearic acids [11]. Due to its vast properties, it has a wide range potential applications: it can be used in the cosmetic industry as an emulsifier, lubricant in the mechanical industry and even for medicinal purposes in the pharmaceutical business [12]. Also, it can also be used as an edible oil, as its fatty acid composition resembles that of olive oil [10].

Up to now, the oil from this plant has been obtained by cold mechanical pressing and conventional solid liquid extraction (SLE) with organic solvents. Both methods present disadvantages, as low extraction yield for the former while, for the latter, a difficult separation of the solvent residue as well as harsh environmental impacts may be cited [13]. As a result, the implementation of a more efficient method to overcome these drawbacks would be advantageous.

Although the end product of the extraction of these two biomasses is the same, the characteristics of the extraction differ significantly: the low extraction yield (<2% wt.) of the *E. crassipes* samples is accompanied by a high concentration of stigmasterol (≅ 15% wt. [9]), whereas for the extraction of *M. oleifera*, due to the high yield of oil obtained (up to 30% wt.), the desired sterol compounds are found in lower concentrations (<1% wt. [13]).

Phytosterols are known to contribute to the minimization of the risk of coronary heart diseases, being thus implemented in a variety of food products. Stigmasterol in particular is widely applied in the pharmaceutical industry where it is employed as a precursor for vitamin D3, cortisone, androgens, estrogens and progesterone [24,25]. Apart from its known industrial uses, stigmasterol has been recently employed with success in many research studies [25,26], where it has been demonstrated this compound may aid in the prevention of several cancer diseases, namely ovarian, prostate and breast types [27].

Stigmasterol is also known for its use in medicinal herbs due to its physiological properties. In fact, this compound inhibits cholesterol biosynthesis in the human body, reducing the concentration of low densities lipoproteins (LDL) and thus, decreasing the risk of heart diseases. A method of producing a stigmasterol derivative salt has been developed by *Kong Chung Oh* [28]. This compound is applied in the treatment of hyperlipidemia and inhibit obesity by reducing the triglycerides content, total cholesterol and LDL-cholesterol in blood. It also increases the concentration of HDL-cholesterol and suppresses an increase in body weight.

Overall, the isolation of phytosterols from natural extracts and residues is a well-known goal in which several processes are described in the literature [21]. The most commonly used methods range from adsorptive [29], to chemical reaction and separation [30], and also thermodynamic fractioning [31] natures. As a result, the possibility of an efficient recovery of this high value products allows the application on a vast field of industries, ranging from pharmaceutical (in the production of therapeutic steroids), nutritional (additives in the food industry) and cosmetics [21].

In this way, the broad field of applications of stigmasterol in the health care industry supports the forthcoming valorization of phytosterol resources, promoting the development of newer and more efficient methodologies that aim at the recovery of this compound.

1.2. Soxhlet extraction

Solid-liquid extraction of is one of the most ancient methods used in the pretreatment of solid samples, being the Sohxlet technique the most widely used for a long time [32]. For over a century, Soxhlet has been the standard procedure and even nowadays is used as comparative purposes for newer methods that rises.

In a conventional process - Figure 2 -, the solid sample is placed in a cartridge holder which is gradually filled with solvent freshly condensed that comes from a distillation flask. When the liquid reaches the maximum height, a siphon aspirates the liquid from the cartridge and unloads the liquid with the extracted analytes in the distillation flask. This process is further repeated until complete extraction is achieved.

In an overall view of the process, the several advantages that this method provides are: (I) the sample is continuously in contact with fresh solvent from the distillation flask, improving therefore the mass transfer equilibrium; (II) the temperature of the system is maintained relatively high throughout the extraction since the solvent is mainly at boiling temperature; (III) no filtration is required for the sample after the extraction; (IV) due to the low cost of the equipment, several extractions can be performed in parallel, increasing the sample throughput; and (V) little training is required for the operation of the equipment due to the simplicity of the process.

On the other hand, the major drawbacks that Soxhlet extraction present regarding other extraction methods the long time required for the conclusion of an extraction and the large amount of solvent wasted, which can also be expensive to dispose, as well as causing environmental issues. Also, due to the extraction being performed at boiling point conditions, thermal sensitive compounds in the solid matrix can be decomposed.

Nevertheless to this several advantages and disadvantages, the Sohxlet apparatus is still widely used mainly to the accessibility and also in order to attain initial information from a new solid sample that requires characterization.

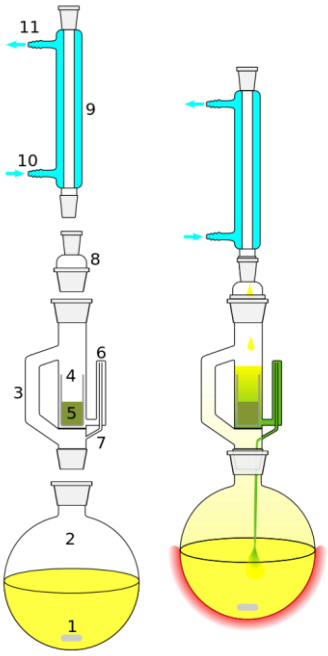

Figure 2 - Soxhlet apparatus scheme. 1 – Solvent; 2 – Still pot; 3 – Distillation path; 4 – Cartridge; 5 – Biomass; 6 – Siphon; 7 – Siphon exit; 8 – Expansion adapter; 9 – Condenser; 10 – Cooling water inlet; 11 – Cooling water outlet

1.3. Supercritical Fluids

Any fluid beyond the thermodynamic vapor liquid critical conditions of pressure (P_c) and temperature (T_c) is usually defined as a supercritical fluid (SCF). At these conditions a distinction between the liquid and gas is not yet observable, being replaced by a single homogeneous phase instead, as illustrated in Figure 3 for the case of carbon dioxide.

Fluids under this state provide a broad range of applications due to their unique and attractive properties, such as low viscosity, high diffusivity, zero surface tension and high compressibility [33]. As a result, supercritical fluids exhibits advantages over the liquid phase by improving mass transfer due to the lower viscosities and higher diffusivities, and over the gas phase by an increase of density providing higher molecular interactions [34]. Table 2 shows a comparison of the order of magnitudes of several properties of SCF with liquids and gases and Table 3 compares the physical properties of supercritical carbon dioxide ($SC-CO_2$) with different solvents.

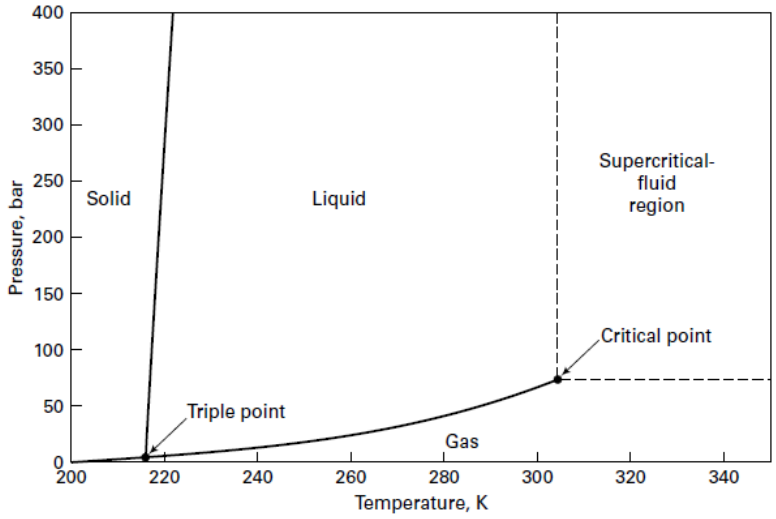

Figure 3-Carbon dioxide phase diagram [35]

Table 2- Comparison of typical values of transport properties in under different physical states.

	Gas	SCF	Liquid
$\rho\ (\mathrm{g \cdot cm^{-3}})$	10^{-3}	0.5	1
$D_{12}\ (\mathrm{cm^2 \cdot s^{-1}})$	10^{-1}	$10^{-4} - 10^{-3}$	$< 10^{-5}$
$\mu\ (\mathrm{g \cdot cm^{-1} \cdot s^{-1}})$	10^{-4}	$10^{-4} - 10^{-3}$	10^{-2}

Table 3- Comparison of physical properties of supercritical carbon dioxide ($\mathrm{SC-CO_2}$) at 200 bar and 55 ºC, with usual liquid solvents at 1 bar and 25 ºC [34].

	$\mathrm{SC-CO_2}$	n-Hexane	Methylene Chloride	Methanol
$\rho\ (\mathrm{g \cdot cm^{-3}})$	0.746	0.660	1.326	0.791
$\nu \times 10^7\ (\mathrm{m^2 \cdot s^{-1}})$	1.00	4.45	3.09	6.91
$D_{12} \times 10^9\ (\mathrm{m^2 \cdot s^{-1}})^*$	6.0	4.0	2.9	1.8

*D_{12} refers to the diffusivity of Benzoic acid in the respective solvents

The concrete application of SCF requires an understanding of multiphase equilibrium at high pressure and the design concepts for technical components in order to apply in industrial plants. Over the past 30 years, significant advances in its use in process media and in the understanding of the interactions with several materials have been made [33]. SCF have been proposed for the application of oil recovery, emulsion splitting, enhanced gas recovery, bitumen separations, among many others applications. One specific application of SCF is in the energy production, where these fluids show prospective features in (I) power generation/refrigeration; (II) biomass conversion for biofuel

generation; (III) reducing environmental impacts; (IV) generation of new materials with increased thermal insulation properties; and (V) process and operation improvements [33].

Nowadays, one of the main applications of SCF is in the field of solid-liquid extraction. Instead of using the typical organic solvents, the solvent applied in this process is a supercritical fluid, being therefore referred as "Supercritical fluid Extraction" (SFE). In this method, the mobile phase is submitted to pressures and temperatures above its critical point in order to attain the supercritical state, hereinafter proceeding to the extraction [34,36,37].

The main advantage in the use of SCF as solvents is in the replacement of the organic counterparts, thus reducing the environmental footprint of conventional processes [33] and promoting the use of green technologies [34].

Apart from the environmental point of view, the properties of the SCF promotes an enhanced process productivity by an increase in the extraction rate and higher selectivities. The main reason relies in the possibility to tune the physical properties by adjusting the operating conditions (P and T), therefore enhancing the responses as desired. However, at conditions in the vicinity of the critical point, such tuning can be difficult since small variations on the operating conditions usually lead to sudden changes in the fluid properties, as shown in Figure 4.

When choosing the ideal solvent to be used in SFE, the most important criterions to take in consideration are [38]:

(I) Selectivity: the solvent should dissolve the desired analyte better than any other compound present in the sample;

(II) Have high retention capacity for the said substance, and thus minimizing the volume required for the extraction;

(III) Be stable and unreactive under the process conditions;

(IV) Un-toxic;

(V) Whenever possible, must have a low cost of purchase.

Typically, the most widely used solvent for SFE is $SC-CO_2$. This choice recalls in the several advantages that CO_2 offers: apart from the previously mentioned, it is also non-flammable, has a low critical point and is easy separable from the sample. Alongside this benefits, the solvent behavior of $SC-CO_2$ can be adjusted with the process conditions, allowing it to resemble the most common organic solvents used, as shown in Table 3.

Due to the vast benefits of this process, SFE using $SC-CO_2$ as solvent is being increasingly used in the scope of obtaining vegetable oils from the respective matrices [5]. In this field, since the extracts are largely composed by components known to be thermal sensitive, low process temperatures must be used, making this solvent perfectly fitted for this purpose - it not only enables

the use of relatively low temperatures due to the low critical point, but also promotes a chemically inert medium in order to avoid possible oxidation of the fatty acids present in the extracts.

Generally speaking, $SC-CO_2$ solvent power can be related to the density by the Hildebrand solubility parameter (δ) defined by Equation (1). In this way, it is possible to establish a preliminary comparison between solvents as long as the solute remains the same. Specifically for supercritical solvents, Giddings et al proposed the following correlation for the Hildebrand solubility parameter as a function of the critical pressure and density [39]:

$$\delta = 1.24 \times P_c^{1/2} \times \frac{\rho(P,T)}{\rho_{eb}(P_{eb},T_{eb})} \quad (1)$$

where $\rho(P,T)$ is the density of the solvent at pressure P and temperature T and ρ_{eb} is the density at boiling point conditions.

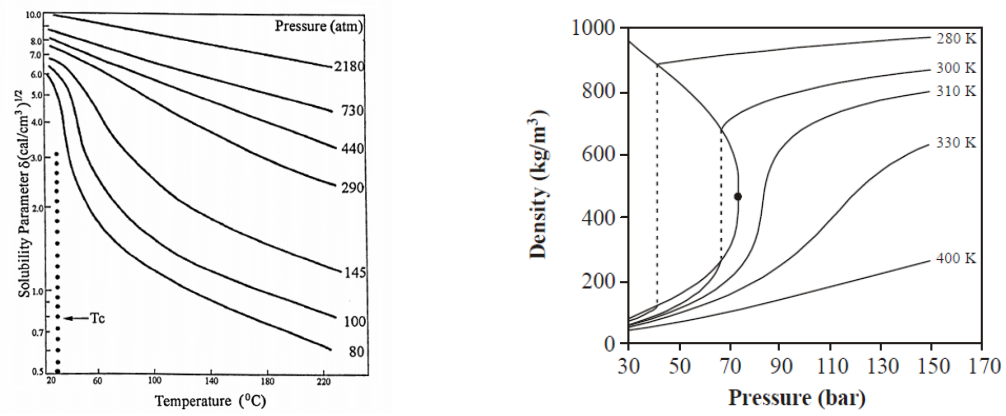

(a) (b)

Figure 4- (a) Effect of Temperature and Pressure on Hildebrand Solubility parameter of $SC-CO_2$ [38] and (b) CO_2 density-pressure diagram [37]

The low critical properties of CO_2 (31°C and 72.9 bar) allows not only the extraction of most compounds without denaturing, but also an easy separation from the sample by thermal expansion, where the pressure of the system is adjusted in a way that promotes the evaporation of the solvent. Furthermore, the polar nature of this solvent can also be adjusted by adding small quantities of modifiers, like methanol and ethanol, thus enhancing the extraction efficiency and also expanding the range of extracts obtained - see Table 4.

Table 4- Solubility enhancements of various solutes in SC-CO_2 with various modifiers[34]

Solute	Modifier	Enhancement Factor = observed solubility/ideal gas solubility
Acridine	3.5% MeOH	2.3
2-Amino benzoic acid	3.5% MeOH	7.2
Cholesterol	9% MeOH	100
Hydroquinone	2% Tributyl phosphate	>300

The overall mass transport stages in a SFE process comprises the solubilization of the extractives in the SCF inside the biomass solid particles, the intraparticle diffusion of the extractives within the supercritical fluid medium, and the final transfer of the extractives from the particle to the bulk supercritical medium from where it is removed from the extractor vessel. With these 3 stages in mind, the interpretation of the extraction curves profiles allows the identification of the rate determining step (RDS) of the process, which is a key knowledge for a correct understanding and project of the phenomena. Examples of generic extraction curves profiles are illustrated in Figure 5. Accordingly, Figure 5 (a) represents a typical extraction curve where the RDS is the solubility of the extractives in the SCF. Since most of the extractives are recovered initially, the overall process occurs at very high rate and low extraction times are needed. On the other hand, in Figure 5 (b), the RDT is the intraparticle diffusion of the compound through the pores of the solid matrix, which implies a more steady and lengthy extraction rate. In Figure 5 (c), the extraction profile is and intermediate between those that are solubility (a) and intraparticle diffusion controlled (b), being the two phenomena simultaneously significant for the rate of the extraction.

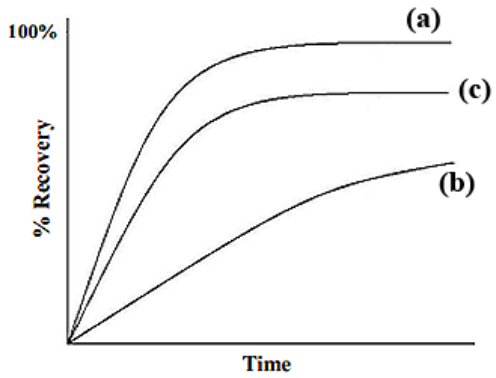

Figure 5- Generic cumulative SFE profiles.

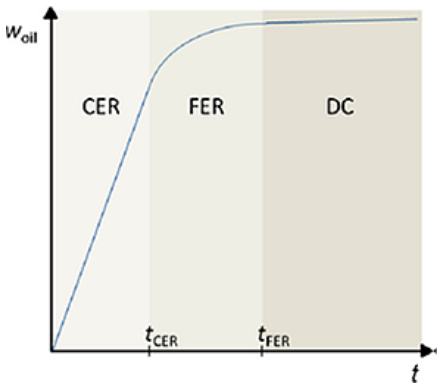

Figure 6-Scheme of the systematized SFE periods.

Taking into account the aforementioned profile possibilities and the reasons for their existence, it is usual to systematize the different extraction periods within a given extraction curve which are related to distinct mass transfer limitations. These allow an instructive characterization of the SFE processes and opens the way to phenomenological modeling – Figure 6. The first extraction period is usually defined as a constant extraction rate (CER) and is marked by the dominance of solubility of the extractives in the SCF. Within this period, which last until reaching the characteristic time t_{CER}, the solubility of the extractives can be calculated, being defined by the slope of the curve in that region, but for this to be valid, no accumulation along the bed nor film limitations should be present. The intermediate region is known as falling extraction rate period (FER) and is the moment when both external and internal mass transfer limitations share importance for the rate of the process. The end of FER period is identified by the characteristic time t_{FER}, which at the same time sets the beginning of the last region, known as diffusion controlled period (DC). The latter represents a moment of lower availability of extractives in the more accessible outer layers of solid matrix, making the process rely in the migration of extractives to the bulk through intraparticle diffusion. Figure 6 illustrates the three common periods on which SFE curves might be systematized: CER, FER and DC.

Due to the abundance of vegetable biomass sources studied by SFE technology, different focus have been reported in the literature [5], the identification of whether dealing with an essential oils or a typical edible oil is a matter of importance. Regarding this subject, essential oils typically contain specialty components but the overall process is known to have a low extraction yield (e.g. <10% wt.). Regarding the extraction of edible oils, these are known for having high extraction yields (e.g. >10%) but low concentration of special compounds such as sterols or others. Although oils have a specific market value in food and cosmetic industries, if SFE processes seek the production of specialty chemicals rather than generic oils, a larger number of non-desirable components are typically removed in these cases, leading to low concentrations of the targeted molecules. In addition, from a mass transport perspective the SFE from vegetable matrices are, for the case of essential oils (low extraction yields), typically governed by internal mass transfer resistances, while for the edible oils (high extraction yields) the limiting step of the extraction is usually the solubility of the extractives, due to reaching the saturation of the SC-CO_2 [5].

Essential oils are well known to have a large number of applications in the pharmaceutical and cosmetic industry due to their physiological and organoleptic properties. Recently, it has been reported the removal of these compounds through SFE in more than 300 species, majorly from seeds and leaves [5,36]. The typical families of compounds usually present in these extracts are phenolics, terpenoids, phytosterols, fatty alcohols and fatty acids.

Over the past 20 years, the use of $SC-CO_2$ has been transferred from the laboratory to a commercial reality in the field of high value products in the pharmaceutical industry, nutraceutical and bulk commodities [33]. Owing to the increase of know-how and development regarding SFE, process integration with other unit operations is a pertinent issue, aiming at further increasing profitability and thus fully taking advantage of all the possibilities that this technology offers. As an example, purification stages can be implemented after the SFE stage in order to recover compounds with added value (such as phytosterols) from the raw extracts/oil, which does not necessarily decreases the commercial value of the raw extract/oil originally produced. This integration approach is currently at early stages of implementation, since the studies performed so far tended to focus solely on the unit operations per se and not as an integrated system [40–45].

1.4. Modeling of the SFE experimental data

1.4.1. Solubility predictive models

Apart from the Hildebrand solubility parameter referred previously that can only provide comparative information of solvent powers, the effective solubility of various compounds on $SC-CO_2$ can be estimated for the desired operating conditions. The most widely used approaches consists on applying equation of state (EoS) and empirical models that can be adjusted to each specific case. Due to the demanding computational effort that EoS requires, the lack of information of physical properties data required for this approach and due to the un-reproducibility of experimental results for high molecular weight compounds, the EoS approach is commonly replaced by simpler empirical models [46].

As a result, the measurement of the solubility of vegetable oils in $SC-CO_2$ through empirical models is mainly dependent on the solvent density at given operating conditions. Thus, the empirical models are commonly known as density based models and describe the behavior of the oil solubility as a function of density and temperature. The seminal correlation proposed by Chrastil (1982) [47] is the most popular model for the solubility estimation [46] and considers the existence of a solvate-complex between the solute molecules and the $SC-CO_2$ at equilibrium, as follows:

$$y^* = \rho^{k_1} \times \exp\left(a_1 + \frac{a_2}{T}\right) \quad (2)$$

where y^* is the solute solubility in the supercritical solvent ($kg \cdot m^{-3}$), ρ is the solvent density expressed in the same units as the solubility, k_1 is the association number, i.e., it represents the average number of CO_2 molecules in the solvato-complex, the constant a_1 is dependent of the molecular weights of the solute and a_2 (K^{-1}) represents the energy associated to the vaporization

Table 5-Few examples of applications of SFE in Vegetable Matrices [5]

Scientific Name	Common name	Morphological part	Target	η	Operating conditions	Uses	Ref
Capsicum anuum L.	Red pepper	Fruit		0.7 – 2.2%	100 – 500 bar; 40 – 60 °C;	Biotic elicitor	[41]
Coffea arabica	Coffee	Residue	Kahweol	0 – 12%	140 – 190 bar; 40 – 70 °C; 91 $kg_{CO2}\ kg_{sample}^{-1}$		[42]
Eucalyptus Globulus	Eucalypt	Bark	Phenolic	0.28 – 0.51%	300 bar; 50 – 70 °C; 45 $L_{CO2}\ kg_{sample}^{-1}$ EtOH (15 – 20% w/w)	Antioxidant activity	[43]
Solanum lycopersicum L.	Tomato	Skin	Lycopene		335 – 450 bar; 45 – 70 °C; 3 – 40 $kg_{CO2}\ kg_{sample}^{-1}$; 0 – 20% Hazelnut oil		[44]
Vitis vinifera L.	Grape	Solid remains	Polyphenols		350 bar; 50 °C; 45 – 180 $L_{CO2}\ kg_{sample}^{-1}$; MeOH (0 – 7%)	Biological activity	[45]

and solvation of the solute, being defined as $a_2 = \Delta H/\Re$, where ΔH is the total reaction heat (vaporization plus solvation) of the solute, and $\Re$ is the universal gas constant.

After Chrastil's equation (1982) [47], several improvements were performed to this model in order to improve suitability to various circumstances: del Valle and Aguilera (1988) proposed an addition of one more term to the initial equation for a better fitting of experimental data [48]; and Adachi and Lu (1983) performed adjustments to the model in order to increase the range of applicability (higher solubility and higher temperature) of this correlation. In fact, several autors have reported [5,11,46] that the Chrastil equation modified by del Valle and provide more accurate prediction of solubility for vegetable oils. This model is the following:

$$y^* = \rho^{k_1} \times \exp\left(a_1 + \frac{a_2}{T} + \frac{a_3}{T^2}\right) \quad (3)$$

The parameters k_1, a_1, a_2 , and a_3 are constants of Equation (3) and have been obtained through the fitting of experimental data from soybean oil, cottonseed oil, sunflower and corn oil [5,46]. The proposed values for the said parameters given in Table 6.

Table 6 - Proposed values for the parameters of del Valle and Aguilera model (Equation (3)) [5,46]

Parameter	Units	Value
k_1	-	10.724
a_1	K^{-2}	2 186 840
a_2	K^{-1}	-18 708
a_3	-	-40.361

1.4.2. Design of Experiments (DoE) and Response Surface Methodology (RSM)

In SFE, RSM is used as an optimization tool that allows statistical based conclusions and trends from the data acquired in experimental runs. The results obtained can be used to evaluate the significance of different factors studied (typically SFE operating conditions), quantify the respective impact, and to describe combined interactions of the tested variables on the final response. Consequently, optimum operating conditions regarding the studied variables can be obtained for the ranges covered by the experimental data used as input.

Initially, a design of experiments (DoE) is selected. This consists of a plan of experimental runs in order to obtain the maximum information of the process with a minimum use of resources. The most used types of experimental designs are the Box-Behnken Design (BBD), Central Composite Design (CCD), Full Factorial and Fractional Designs. Regarding the choice of the factors to evaluate the SFE process, temperature, pressure, time of extraction/mass of spent solvent and co-

solvent amount are the most commonly studied in SFE [5]. Regarding the DoE, the maximum experimental runs (N) possible to perform in a Full Factorial Design is related to the number of factors (n) and levels of correspondence (k): $N = n^k$.

For the specific case of 2^{nd} degree polynomial fits, the BBD is the most widely used in RSM. It requires at least 3 levels for each factor and it's based in an incomplete DoE whilst producing feasible results. Each run is performed by fixing one factor at its center point and combining the remaining factors in their extreme values, thus eliminating the runs that comprises the combinations of all the factors at their extreme points simultaneously. The last three runs are performed at the central point and aim to understand the variability associated with the experimental procedure, and thus predict the natural trend of each parameter by taking in consideration the occurrence of experimental errors.

In a typical DoE with 3 factors and 3 levels of correspondence, the BBD requires only 15 experimental runs, whereas with a Full Factorial Design, a total of 27 arrangements (3^3) are necessary in order to complete the experimental design. This makes the BBD the most rational method due to the reduced number of runs and, consequently, allowing a lower consumption of time and resources. Table 7 summarizes the recommended experimental arrangements within DoE, based on the number of factors to be included, and the objectives of the study.

Table 7- Recommended Design of experiments guide-line [49]

Number of factors	**Comparative objective**	**Screening Objective**	**Response surface objective**
1	1 factor completely randomized design	-	-
2-4	Randomized block design	Full or Fractional Factorial	Central composite or Box-Behnken
5 or more	Randomized block design	Fractional Factorial	Screen first to reduce number of factors

After performing the experimental assays specified in the chosen DoE arrangement, the following step of the RSM is the adjustment of the data obtained to a mathematical equation that relates the response studied to the process variables, as shown in Equation (4). This step is performed by linear least squares regression, followed by an adequacy test to verify the adequacy of the fit.

$$y = \beta_0 + \sum \beta_{\mathrm{i}} X_{\mathrm{i}} + \sum \beta_{\mathrm{ii}} X_{\mathrm{i}}^2 + + \sum \beta_{\mathrm{iii}} X_{\mathrm{i}} X_{\mathrm{j}} \quad (4)$$

where β_i are the model's coefficients and X_i are the (coded) process variables being evaluated. Since each factor may have distinct orders of magnitude on its original units, it is necessary to perform a change of variables so that every factor has the same ranging interval. This correction is performed using Equation (5) for a 3 levels of correspondence DoE:

$$X_i = \frac{x_i - x_0}{\Delta x} \quad (5)$$

where x_i is the true value of the factor i, x_0 is the middle point of the interval range and Δx is the step between levels of correspondence.

Since RSM is a tool based in statistical modeling, one must be aware that even the best results obtained are merely an approximation to the reality, and even the optimum point obtained may not necessarily represent the best conditions. This is due to the parameters evaluated being accompanied by uncertainty and experimental errors, and therefore the interpretation of the results must be conducted with good judgment. Nonetheless, the responses obtained using this method provide reliable results within the factors value range they cover and refer to.

1.4.3. Economic analysis through cost of manufacturing (COM) approach

Since SFE is a high-pressure alternative technology that competes with classical SLE methods when considering an industrial implementation, the cost of manufacturing (COM) approach can be used as a method to demonstrate the potential and viability of SFE processes.

The economic assessment is performed by the methodology proposed by Turton et al. [50] which has been applied in various works in the last years, such as in the SFE of tomato residues and spent coffee grounds [51,52]. The cost of manufacturing (COM) calculation relies in a general function of the investment cost (FCI), labor (COL), utilities (CUT) waste treatment (CWT) and raw materials (CRM) costs, as follows:

$$\mathrm{COM} = 0.304\mathrm{FCI} + 2.73\mathrm{COL} + 1.23(\mathrm{CUT} + \mathrm{CWT} + \mathrm{CRM}) \quad (6)$$

Despite simple, for an accurate scoring of COM several assumptions need to be considered which are displayed in Table 8.

Since the objective of COM is studying how much would an extract/oil cost if a SFE industrial unit would be used, laboratory data needs to be scaled-up, for which four criteria used based on the rate determining step (RDS) of the extraction process [53]:

(I) if the RDS is the solubility, the ratio between the mass of spent solvent and the quantity of biomass must be held constant ($w_{CO_2} \cdot w_b^{-1}$);

(II) if the process is controlled by diffusion, the ratio of solvent flow rate and the quantity of biomass must be maintained constant ($\dot{Q}_{CO_2} \cdot w_b^{-1}$);

(III) if both of the referred limitations are significant, both criterions must be applied

(IV) Both the criterions might be applied, as well as fixing a dimensional number characteristically of the process (as for example the Reynolds number, Re).

Concerning the initial investment (FCI), typical values for SFE units were recently published in the literature [54]. For example, a unit consisting of two $0.4\ m^3$ extractors, flash tank, CO_2 reservoir, condenser, pump and heat exchanger is priced at 2M$ (US). When information for the required equipment is not available, the cost of purchase can be corrected by multiplying the known value with the ratio of capacity parameters, being this correction usually known as the six-tenth rule [55], as follows:

$$FCI_2 = FCI_1 \times \left(\frac{w_2}{w_1}\right)^{0.6} \quad (7)$$

where FCI_i is the investment cost of extractor i and w_i is the charge that the extractor i holds.

In order to estimate the utility costs (CUT), computational simulations using process softwares like Aspen Plus® are required to obtain a first approximation of the consumption of electricity and steam in the process. The cost associated to the raw materials (CRM) namely biomass pretreatment and CO_2 make-up can be obtained by material and energy balances. Regarding the waste treatment cost (CWT), the absence of relevant atmospheric emissions (CO_2 circulates in closed loop) allows to neglect this parcel in the COM.

1.4.4. Kinetic modeling of the extraction curves

In order to disclose the prevailing mechanism of the extraction process, the experimental extraction curves can be modeled by simple expressions based in material balances (inside the extractor bed and in the particles), disclosing the various mass transfer phenomena present for each case scenario. Considering the several assumptions taken to simplify the said material balances, different models based on the main limitation to the process can then be highlighted, as for example solubility on the supercritical solvent, internal diffusion and even interfacial film resistance. This method is performed by calculating one or more adjustable parameters proposed for each case, being the goodness of the fit evaluated by the average absolute relative deviation (AARD) – Equation (8):

Table 8- List of assumptions concerning the economic study of a SFE process [5]

General	1. Working period; 2. Number of workers *per* extractor; 3. Scale-up criterion; 4. Minimum pressure in the extract collector vessel; 5. Time required to discharge, re-charge and re-pressurize the extractor; 6. Definition of the quantity of CO_2 lost in each cycle due to decompression; 7. Bed density and porosity; 8. Market price of the SFE extract; 9. Sample initial moisture;
FCI	10. Annual depreciation rate; 11. Price of the SFE unit;
COL	12. Labor cost;
CUT	13. Electricity cost; 14. Steam cost;
CWT	15. Waste treatment cost;
CRM	16. Matrix drying treatment, milling and other pretreatment cost; 17. Make-up CO_2 purchase cost.

$$\mathrm{AARD}(\%) = \frac{100}{\mathrm{n}} \times \sum_{i=1}^{n} \left| \frac{\eta_{\mathrm{i}}^{\mathrm{calc}} - \eta_{\mathrm{i}}^{\mathrm{exp}}}{\eta_{\mathrm{i}}^{\mathrm{exp}}} \right| \quad (8)$$

where n is the number of points of the extraction curve, $\eta_{\mathrm{i}}^{\mathrm{exp}}$ and $\eta_{\mathrm{i}}^{\mathrm{calc}}$ are the experimental and calculated extraction yield, respectively. For that purpose, three phenomenological models were adjusted to the extraction curves obtained and the respective evaluation of the associated error was assessed. Focusing mainly on two limiting steps of the transport phenomenon, the models hereinafter presented highlight the effects of internal diffusion and interfacial mass transfer, as displayed in the works of marigold [56], eucalypt [57], shiitake [58] and peach [59].

Regarding the diffusion controlled models, they assume that the limiting stage of the process is the intra particle transport, being the overall extraction profile similar to the third period of extraction (DC) displayed in Figure 6. Gaspar et al. [60] presented the Simple Single Plate model (SSPM – Equation (9)). This model assumes particles with plate geometry and that mass transfer resistance in the fluid phase is neglected, being the process therefore governed by intraparticle diffusion:

$$\eta(t) = X_0 \times \left[1 - \sum_{n=0}^{\infty} \frac{0.8}{2n+1} \exp\left(-\frac{D_m}{\theta^2}(2n+1)^2\pi^2 t\right)\right] \quad (9)$$

where η ($\mathrm{kg_{solute}}$ per 100 $\mathrm{kg_{biomass}}$) is the extraction yield, X_0($\mathrm{kg_{solute}}$ per 100 $\mathrm{kg_{biomass}}$) is the total extractable amount available in the biomass, D_m ($\mathrm{m^2 \cdot h^{-1}}$) is the effective diffusivity and θ (m) is the plate thickness, being the ratio D_m/θ^2 the fitting parameter of this model.

The Diffusion Model (DFM) – Equation (10) – proposed by Crank [61] for spherical geometries assumes that intra particle diffusion is the main resistance to the transport of the molecules to the fluid phase. Similarly to the SSPM model, the fitting parameter is the ratio between the effective diffusivity and the particle radius, D_m/r^2.

$$\eta(t) = X_0 \times \left[1 - \frac{6}{\pi^2} \sum_{n=1}^{\infty} \frac{1}{n^2} \exp\left(-\frac{D_m}{r^2} n^2\pi^2 t\right)\right] \quad (10)$$

Cocero and García [62] proposed a phenomenological model that describes the extraction process by a linear equilibrium together with film resistance to the mass transport (LEFM). In general, the following hypotheses were considered for the description of the extraction system:

(I) a pseudo component is considered and is representative of the global behavior (being defined as "solute" – however, the referred model can also be applied to singular components and the conclusions obtained remain valid);

(II) the extraction system is considered as fixed bed with two different phases – static solid phase (in which the matrix holds the desired compounds to be removed) and a mobile fluid phase (composed as supercritical fluid, co solvent and solute);

(III) solvent flow rate and physical properties (as density and viscosity) remain constant through the extraction process (pressure drop and temperature gradients are neglected);

(IV) Superficial velocity is constant and may be calculated solely considering the supercritical fluid flow rate (co-solvent flow rate is neglected); bed porosity is constant along the extractor bed;

(V) axial and radial dispersion are neglected in order to further simplify the model. It is worth to notice that this last simplification does not invalidate the model, because the introduction of this two parameters increases the model degrees of freedom and therefore provides a better fitting.

The material balances in the solid matrix and supercritical fluid can be written as follows:

$$\begin{cases} \varepsilon \times \dfrac{\partial y}{\partial t} = -u \times \dfrac{\partial y}{\partial z} - k_{\mathrm{f}} a_0 (y - y') \\ (1-\varepsilon)\rho_{\mathrm{s}} \dfrac{\partial y_{\mathrm{s}}}{\partial t} = (k_{\mathrm{f}} a_0)(y - y') \\ y_{\mathrm{s}} = H y' \end{cases} \tag{11}$$

where u ($\mathrm{m} \cdot \mathrm{h}^{-1}$) is the superficial velocity of the fluid phase (assumed constant throughout the extraction process, and calculated by $u = \dot{Q}_{\mathrm{CO_2}}/(\rho_{\mathrm{CO_2}} \times S)$, where S (m^2) is the extractor cross section), H is the partition coefficient regarding equilibrium, y_{s} ($\mathrm{kg} \cdot \mathrm{kg}_{\mathrm{biomass}}$) is the solute concentration in the solid phase, y ($\mathrm{kg} \cdot \mathrm{m}^3$) is the solute concentration in the fluid phase, $y'(\mathrm{g}_{\mathrm{solute}} \cdot \mathrm{cm}^{-3}_{\mathrm{solid}})$ is the surface equilibrium concentration, ρ_{s} ($\mathrm{kg} \cdot \mathrm{m}^{-3}$) is the solid density, ε is the bed porosity and z (m) is the axial coordinate in the fixed bed. The initial and boundary conditions required in order to solve the system of partial differential equations are: for $t = 0 \rightarrow y = 0$ and $y_{\mathrm{s}} = X_0$; for $z = 0 \rightarrow y = 0$. The yield values are estimated by an overall mass balance to the whole system:

$$\eta(t) = 100 \times \frac{\dot{Q}_{\mathrm{CO_2}}}{\rho_{\mathrm{CO_2}} w_{\mathrm{b}}} \int_0^t y(t, z = L_{\mathrm{b}}) \mathrm{dt} \tag{12}$$

where L_{b} (m) is the bed length, $\dot{Q_{\mathrm{CO_2}}}$ ($\mathrm{kg} \cdot \mathrm{h}^{-1}$) is the supercritical solvent flow rate, w_{b} (kg) is the extractor load and $\rho_{\mathrm{CO_2}}$ ($\mathrm{kg} \cdot \mathrm{m}^{-3}$) the density of the fluid. Overall, the two adjustable parameters are the mass transfer film coefficient ($k_{\mathrm{f}} a_0$) and the partition coefficient (H). The analytical solution of this model can be obtained using the method of lines (MOL) [63] for discretization in space with 50 finite differences in the axial coordinate. Following this step, the discretized model can then be implemented in Matlab™ and solved using the explicit Runge-Kutta method of 4th and 5th order. Finally, the numerical integration of Equation (12) is performed using the 1/3 Simpson rule.

2. Optimization and modeling of the SFE of *E. crassipes*

In this section, the following studies are presented:

(I) Measurement of nine fixed time SFE assays and their respective statistical optimization (RSM modeling) [16], with the aim of identifying the best operating conditions (pressure, *P*, and ethanol content, x_{EtOH}) to total extraction yield, sterols extraction yield, sterols concentration, and individual sterols concentrations (stigmasterol, cholesterol, and β–sitosterol);

(II) Measurement of six SFE curves and their respective kinetic modeling, upon application for the models presented in subsection 1.4.4. in order to assess the predominant resistance to the mass transport during the extraction.

2.1. Materials and methods

2.1.1. Raw material

E. crassipes samples were obtained at Pateira de Fermentelos (40º 34' 31'' N, 8º 30' 57'' W), Aveiro, Portugal. The desired raw material, namely leaves and stalks, was separated from the remaining biomass and was initially air dried to remove the majority of the moisture. A mixture of these two morphological parts was produced under a known ratio comprising 65% (wt.) of leaves and 35% (wt.) of stalks. Subsequently, the samples were submitted to a drying stage in a ventilated oven at 35 ºC. The dried samples were then grinded and further dried until no mass difference was achieved in order to quantify the biomass natural moisture.

2.1.2. Soxhlet and SFE extraction

Soxhlet extractions with dicloromethane were performed in duplicate in order to establish a reference composition of the extracts for the supercritical fluid extractions

Samples of approximately 16.6 grams were place in the Soxhlet cartridge and were submitted to a 6 hours extraction, after which the solvent was evaporated to dryness. The total extraction yield, total sterols yield ($\eta_{\mathrm{TotalSterols}}$), individual yields ($\eta_{\mathrm{i}}$) and individual concentrations (C_{i}) were calculated with the following expressions:

$$\eta_{\mathrm{Total}}(\mathrm{wt.\,\%}) = \frac{w_{\mathrm{extract}}}{w_{\mathrm{biomass}}} \times 100 \qquad (13)$$

$$\eta_{\text{TotalSterols}}\ (\text{wt.}\%) = \frac{w_{\text{sterols}}}{w_{\text{biomass}}} \times 100 \quad (14)$$

$$\eta_{\text{i}}(\text{wt.}\%) = \frac{w_{\text{i}}}{w_{\text{biomass}}} \times 100 \quad (15)$$

$$C_{\text{i}}(\text{wt.}\%) = \frac{w_{\text{i}}}{w_{\text{extract}}} \times 100 \quad (16)$$

where w_{extract} is the mass of extract, w_{Sterols} is the mass of the total sterol fraction extracted, w_{i} is the mass of an individual extractive molecule, and w_{biomass} is the mass of the dried biomass sample used in the experiment.

The SFE was performed in a Spe-ed™ apparatus (Applied Separations), in which the flow sheet is displayed in Figure 7, where an approximate load of 30 g of sample was introduced in the extractor.

Overall, the liquid CO_2 is pressurized by a cooled liquid pump to the desired extraction pressure. It follows a heating stage before the extraction column where the solvent is heated to the extraction temperature. After attaining the supercritical state, the solvent flows upwards through the extractor were the biomass was previously placed. Following the percolation of the solvent through the vessel, the extract stream is then depressurized by a heated back pressure regulator valve (BPR) and bubbled in ethanol as to capture the extract removed from the sample for subsequent yield quantification and characterization. Finally, the spent CO_2 is vented to the atmosphere. Regarding the SFE assays with modifiers, the addition of co-solvent is accomplished by a liquid pump (LabAlliance Model 1500) coupled to the CO_2 line between the mass flow meter and the heating vessel.

The experimental runs performed and the respective operating conditions are summarized in Table 9. It was adopted a Full Factorial DoE for the optimization study with 2 factors and 3 levels of correspondence (Table 10), totaling 9 experimental runs (3^2). The temperature was fixed on 50 ºC, which is well between the common range usually found in SFE of vegetable biomass [5].

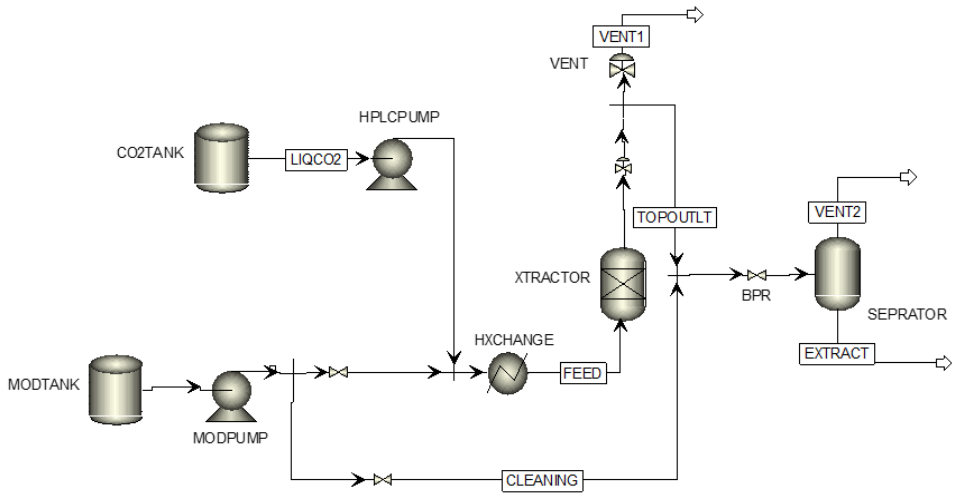

Figure 7 - Flow sheet of the SFE set up used to produce the experimental data

Table 9 - Operating conditions of the SFE of *E. crassipes*

Experiment	Type	*P* (bar)	*T* (ºC)	$\dot{Q}$ ($g \cdot min^{-1}$)	x_{EtOH}
Run 1	Curve	200	50	7.5	0.0
Run 2	Curve	250	50	7.5	0.0
Run 3	Single point	300	50	7.5	0.0
Run 4	Single point	200	50	7.5	2.5
Run 5	Single point	250	50	7.5	2.5
Run 6	Single point	300	50	7.5	2.5
Run 7	Single point	200	50	7.5	5.0
Run 8	Curve	250	50	7.5	5.0
Run 9	Curve	300	50	7.5	5.0
Run 10	Curve	250	50	5.0	0.0
Run 11	Curve	250	50	10.0	0.0

Table 10 - Codification and levels of correspondence of the variables considered for the DoE

Factor	Variable	Level of correspondence		
		-1	0	+1
Pressure (bar)	$X_P = (P - 250)/50$	200	250	300
Ethanol content (%)	$X_{EtOH} = (x_{EtOH} - 2.5)/2.5$	0.0	2.5	5.0

2.1.3. Gas chromatography – Mass spectrometry (GC-MS)

Beforehand the GC-MS analysis, approximately 20 mg of each extracted sample were converted into its trimethylsilyl counterpart [64]. The procedure that was applied is as follows: each dried sample was dissolved in 250 μL of pyridine containing 1 mg of tetracosane. The addition of 250 μL of N,O-bis(trimethylsilyl)trifluoroacetamide and 50 μL of trimethylsilyl chloride promotes the conversion of compounds with hydroxyl and carboxyl groups to trimethylsilyl (TMS) ethers and esters, respectively. This mixture was then maintained at 70 ºC for 30 minutes [4]. Finally, each extract was analyzed in duplicate with tetracosane as internal standard.

The equipment used was a Trace Gas Chromatograph 2000 Series equipped with a Finnigan Trace MS mass spectrometer, using helium as carrier gas (35 cm s^{-1}), equipped with a DB-1 J&W capillary column (30 m × 0.32 mm i.d., 0.25 μm film thickness) and coupled with an auto-sampler. The chromatographic conditions were as follows: initial temperature: 80ºC for 5 min; heating rate: 4 ºC min^{-1}; final temperature: 285 ºC for 10 min; injector temperature: 250ºC; transfer-line temperature: 290ºC; split ratio: 1:50. The MS was operated in the electron impact mode with electron impact energy of 70 eV and data collected at a rate of 1 scan s^{-1} over a range of m/z of 33–750. The ion source was maintained at 250ºC.

For the quantitative analysis, the instrument was calibrated with a pure reference compound representative of the family of compounds desired to quantify (β-sitosterol), relative to the internal standard. The response factor necessary to obtain correct quantification of peak areas was calculated as a mean of two-three GC-MS runs.

2.2. Results

2.2.1. Characterization of the extracts obtained by Soxhlet and SFE

At an initial stage, the characterization of the extracts obtained either by conventional methods such as Soxhlet and SFE was assessed with the aim of quantifying and comparing the extractives obtained by each approach. Figure 8 represents a typical GC-MS chromatogram of a dichloromethane Soxhlet extraction where the sterols retention times (RT) are outlined. Due to the vast amount and high concentration of stigmasterol present in the extract, and due to being the most valuable compounds in the extract, the overall sterol family was specifically emphasized in this work. The extraction with the organic solvent led to a total extraction yield of 1.9% wt. with the total sterols fraction comprising 23.7% (wt.%) of the global extract. In addition, the individual concentration of stigmasterol, cholesterol, β-sitosterol, and methylcholesterol in the extracts amount 15.55%, 3.50%, 2.98%, and 1.67%, respectively. These Soxhlet extraction results were taken as reference values along the SFE optimization carried out. Table 11 also provides the characterization of one SFE assay

from the optimization series, namely Run 7, allowing a direct comparison between the two extraction methods. In this sense, although the total extraction yield obtained by SFE for the selected conditions (η_{Total}= 0.75% wt.) is far lower than the value obtained by the conventional extraction method (η_{Total}= 1.9% wt.), the SFE assay provides a far more selective extraction of the sterols family, reaching a concentration of 36.6% , a value that is 1.5 times higher than those obtained by Soxhlet whith dichloromethane..

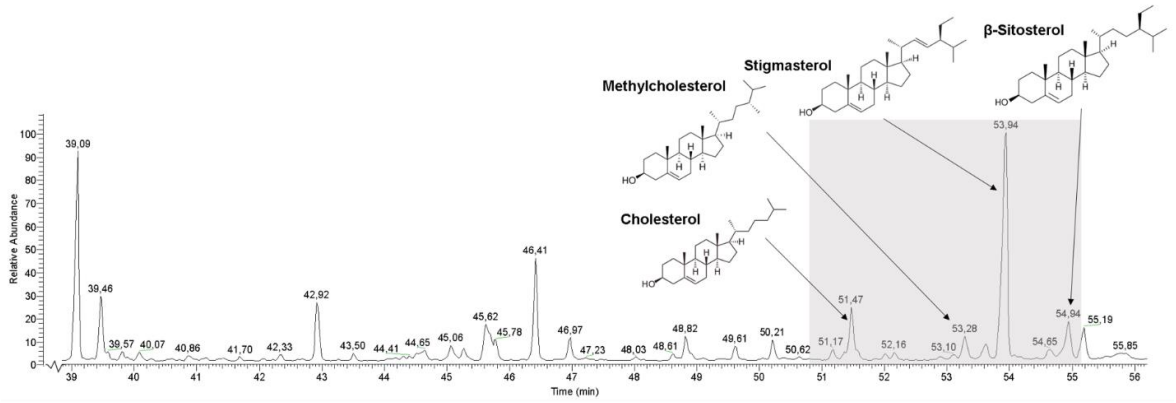

Figure 8 - GC–MS chromatogram of a dichloromethane extract of *E. crassipes*. The sterols of interest are found within the delimited region.

Table 11- Identification and quantitative determination of sterols in the dichloromethane and supercritical CO_2 extracts of *E. crassipes*

Peak	RT (min)	Compound	Soxhlet		SFE (300 bar, 0% EtOH)	
			η_{i} ($\mathrm{mg \cdot kg_{biomass}^{-1}}$)	C_{i} (wt. %)	η_{i} ($\mathrm{mg \cdot kg_{biomass}^{-1}}$)	C_{i} (wt.%)
1	51.47	Cholesterol	681.1	3.5%	346.6	4.6%
2	53.28	Methylcholesterol	325.0	1.7%	177.5	2.4%
3	53.94	Stigmasterol	3023.8	15.6%	1889.0	25.1%
4	54.94	β-sitosterol	579.9	3.0%	339.2	4.5%
Total Sterols ($\mathrm{mg \cdot kg_{biomass}^{-1}}$)			4609.8	23.8%	2752.3	36.6%
(wt.%)			0.46%		0.28%	
Total Yield (wt.%)			1.90%		0.75%	

2.2.2. Preliminary measurement of extraction curves

Due to the large number of process parameters (and values) that can be chosen for a optimization study, a criteria must be established in order to choose which variables are going to be submitted to the evaluation, and which are going to be fixed at constant value. With the aim to disclose the factors to be evaluated in the optimization study, several extraction runs were performed and the individual effect of each parameter was qualitatively analyzed.

By maintaining constant the operating conditions *P*, *T*, and x_{EtOH}), the impact of the flow rate in relation to the total extraction yield was assessed. Figure 9 (a) presents three cumulative extraction curves (normalized regarding η_{Total} obtained by Soxhlet extraction) for the flow rates of 5.0, 7.5 and 10.0 g min^{-1}, respectively. At a first insight, a 10% increase in the total extraction yield is observed when passing from the lowest flow rate (5.0 g min^{-1}) to 7.5 g min^{-1}. On the other hand, for the flow rate increment from 7.5 to 10.0 g min^{-1}, only a 3.2% increase in the total extraction yield is obtained.

Since the direct effect of the flow rate is felt on the hydrodynamics of the process, and taking into account that the remaining operating conditions (P, T, x_{EtOH}) did not vary, the enhancements caused by the increase of the flow rate over η_{Total} are exclusively due the reduction of the external film layer, i.e. the interface resistance formed between the external layer of solid particle and the bulk medium. By noticing the slow enhancement attained in flow rate increment (7.5 to 10.0 g $\cdot$ min^{-1}), an additional increase in the turbulence of the process is not expected to decrease the film resistance any further.

Through an empirical correlation the prediction of the percentage increase of the mass transfer film coefficients at fixed conditions (k_{f}) due to the increase of the flow rate [65] can be calculated as follows:

$$\frac{(k_{\mathrm{f}})_2}{(k_{\mathrm{f}})_1} = \left(\frac{\dot{Q}_2}{\dot{Q}_1}\right)^{0.8} \tag{17}$$

Between the lowest flow rates, when passing from 5.0 to 7.5 g min^{-1}, an increase of 38% in the k_{f} is observed, whereas only a 26% increase is detected when passing from 7.5 to 10.0 g min^{-1}. The reduced increment in the mass transfer coefficient, accompanied to the fact there has not been observed a notable gain in the extraction yield when passing from the intermediate flow rate to the maximum studied, point towards to the elimination of the film resistance and the move to a process controlled by intraparticle diffusion. In section 2.2.5 – Modeling of the extraction curves, this assumption is further discussed through the application of simplified models with different mass transport assumptions.

Regarding the modifier content, two SFE curves were measured (Run 2 and Run 8) in order to verify the impact in the total extraction yield due to the increase of polarity of the supercritical solvent. For the conditions of 250 bar, 50 ºC and for the flow rate that eliminates the major film resistances (previously identified as being 7.5 g min^{-1}), it was observed – Figure 9 (b) – that 5.0% of the modifier content (Run 8) increases the total extraction yield up to 1.6 times. As a result, it was decided to include the co-solvent content in the SFE optimization study.

As far as stigmasterol concentration is concerned, the respective cumulative profiles are present in Figure 10 for the 4 extraction curves under analysis. When interpreting the extraction curves in terms of stigmasterol concentration, a notorious trend may be observed when comparing the SFE results with the data obtained by the Soxhlet reference result. Overall, any point of the SFE curves is more concentrated in stigmasterol than under Soxhlet extraction with dichloromethane, ranging this increment from 1.19 times (Run 8 at t = 6h), to 1.72 times (Run 8 at t =1h). Remarkably conditions of Run 8, i.e. 250 bar, 50 ºC, 5.0% EtOH and $\dot{Q}$ =7.5 g min^{-1} provided the maximum and the minimum C_{stigm} values. In fact, the inflection observed from the cumulative concentration profiles denotes the existence of an optimum extraction time to maximizes the concentration of stigmasterol in the final extract (especially for the scenario where co-solvent is used).

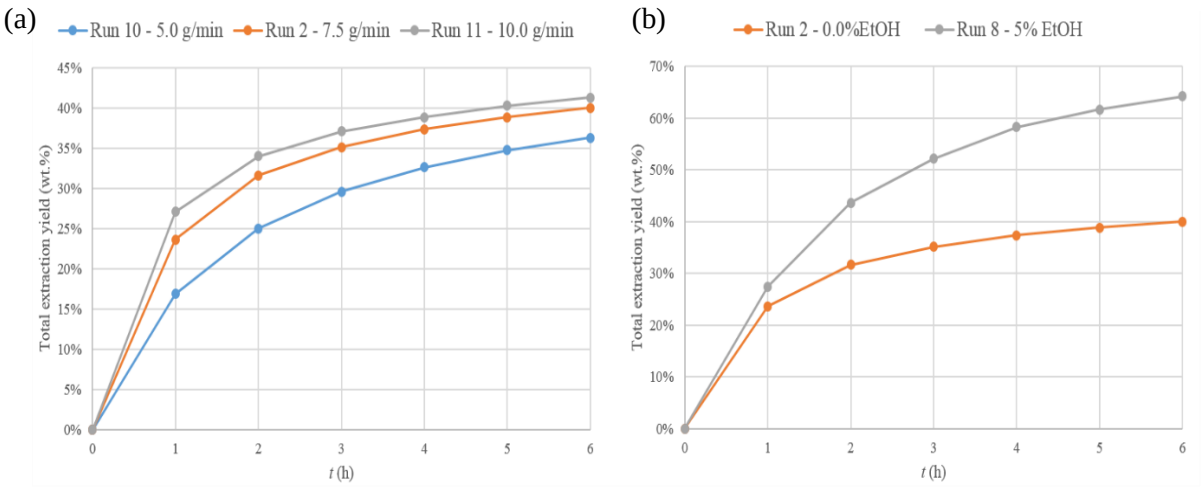

Figure 9 – Cumulative extractions yield profile curves at (a) different flow rates at 250 bar, 50 ºC, 0.0% ethanol; (b) different ethanol content at 250 bar, 50 ºC, 7.5 g min^{-1}; Results normalized by Soxhlet yield = 1.9% (wt.).

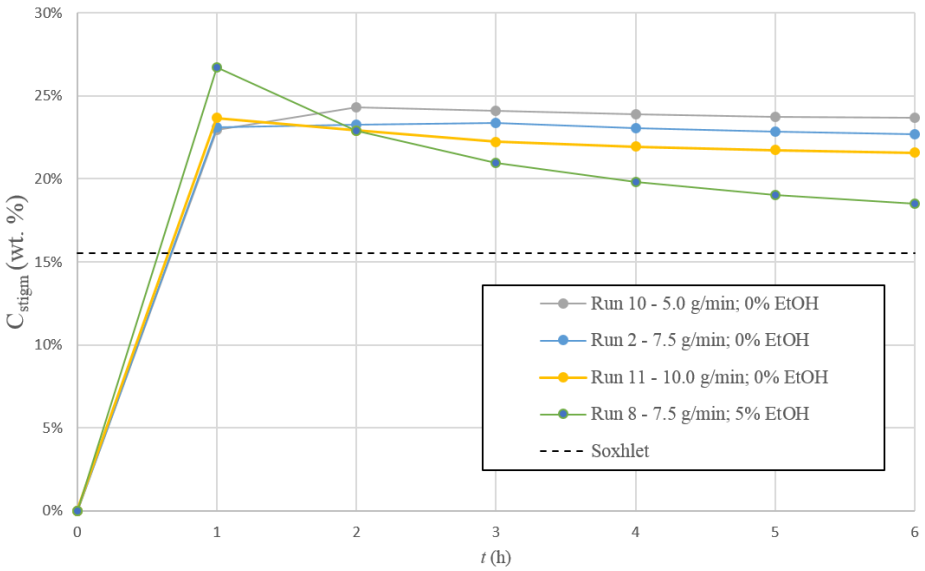

Figure 10 – Cumulative stigmasterol concentration in extracts ($kg \cdot 100kg_{extract}^{-1}$) along time

2.2.3. SFE optimization results

The experimental results of nine extraction assays are displayed in Table 12. Six different responses were optimized in this work, these being total extraction yield (η_{Total}), total sterol extraction yield ($\eta_{\mathrm{TotalSterol}}$), total sterol concentration ($C_{\mathrm{TotalSterol}}$), stigmaterol, β-sitosterol and cholesterol concentration (C_{Stigm}, $C_{\beta-\mathrm{sitost}}$ and C_{cholest}, respectively).

With regard to η_{Total}, the obtained yield ranges from 0.72% (wt.) for the conditions of Run 1 [P=200 bar; x_{EtOH}=0.0% (wt.)] to 1.24% (wt.) for the conditions of Run 9 [P=300 bar; x_{EtOH} =5.0% (wt.)], which correspond to 37 and 65% (wt.) of the reference value given by the Soxhlet extraction yield (1.9% wt.). In terms of $\eta_{\mathrm{TotalSterol}}$: the absolute values of the later ranged from 0.24% (wt.) in Run 4 [P=250 bar; x_{EtOH} =0.0% (wt.)] to 0.35% (wt.) in Run 8 [P=250 bar; x_{EtOH} =2.5% (wt.)]. These represent 52-76% (wt.) of the sterols content established by the Soxhlet reference.

With the aim of investigating the main factors that influence the considered responses in this study, the experimental data was adjusted to quadratic polynomial (with the form of Eq.(4)) and the Full models (FM) obtained are displayed in Table 13, alongside the respective p-values regarding their statistical significance. In order to simplify the predictive model obtained, the coefficients that were statistically significant to the response ($p<0.05$) were preserved and the experimental data points were re-fitted. Considering a general overview of fitting parameters, it is possible to assess the influence of each contribution towards each response. Regarding extraction yields, due to the positive signs of the β coefficients, all terms involving ethanol contribution (β_2,β_4 and β_5) acts towards the increase of the response, whereas for the concentration responses the inverse scenario

occurs. In practice, this implies that ethanol induces an increase of the overall amount of extractives attained but such increment is mainly at the expenses of other compounds than the sought ones. As a results a dilution of the key compounds is prone to be achieved as more ethanol is added to the SC-CO_2.

The coefficients of determination (R^2) and adjusted coefficients of determination (R^2_{adj}), that aid in the understanding of the quality of the adjustment are also displayed. Overall, every response provided R^2 higher than 0.85, being the highest for η_{Total}, attaining a value of 0.98. However, with the exception of η_{Total}, all the other responses exhibit R^2_{adj} values that differ significantly from the R^2, which indicates that the favorable goodness of fit attained in those responses is at the expenses of the several parameters of the full model, even though most of them are shown not to be statistically significant.

The reduced models are shown in Table 14. Although more accurate from a statistical significance perspective, the reduced models of all responses (excepting η_{Total}) exhibit a poor suitability to describe the experimental points, as revealed by the R^2 values not greater than 0.61. This phenomenon is mainly due to the lack of capacity in the models to cope with the fluctuations exhibited by the experimental data. Taking into account that analysis of SFE trends on each response demands models with high enough determination coefficients, for the analysis of next sections the full models rather than de reduced ones, were used.

Table 12- Results of the SFE assays performed for the purpose of the statistical optimization.

Run	P (bar)	%EtOH	η_{Total} (wt. %)	$\eta_{\text{TotalSterol}}$ (wt.%)	Concentration (wt. %)			
					$C_{\text{TotalSterol}}$ (wt. %)	C_{Stigm} (wt. %)	$C_{\beta-\text{sitost}}$ (wt. %)	C_{cholest} (wt. %)
1	200	0	0.72	0.25	35.02	24.90	3.91	4.12
2	200	2.5	0.90	0.30	33.17	22.19	4.19	4.74
3	200	5	1.17	0.31	27.92	18.96	3.62	3.63
4	250	0	0.78	0.24	31.12	22.70	3.67	3.54
5	250	2.5	0.88	0.32	36.32	24.76	4.33	4.89
6	250	5	1.25	0.34	27.28	18.49	3.52	3.48
7	300	0	0.75	0.28	36.63	25.14	4.52	4.61
8	300	2.5	0.90	0.35	38.26	26.35	4.74	4.89
9	300	5	1.24	0.30	24.35	17.59	2.97	2.50

2.2.3.1.Optimization of total extraction yield (η_{Total})

In what concerns trends on η_{Total}, Figure 11 (a) shows the surface of this response along pressure and ethanol content, being perceptible that the contribution of the ethanol fraction in the supercritical solvent provides a higher impact than the overall effect of pressure. In fact, within the studied pressure values range (200-300 bar), relevant solvent properties such as density (ρ) and viscosity (μ) do not vary expressively: for instance ρ(300 bar,50ºC,0.0 wt.% EtOH)/ρ(200 bar,50ºC,0.0 wt.% EtOH) =1.1 and μ(300 bar,50ºC,0.0 wt.% EtOH)/μ(200 bar,50ºC, 0.0 wt.% EtOH) =1.2 . Although ethanol addition can affect per se the density and viscosity of the supercritical phase, Figure 11 (a) evidences that jumps from 200-300 bar at either 2.5 or 5.0 wt.% EtOH are not more pronounced than without co-solvent, which reinforces the idea that relevant properties of the supercritical CO_2 (or mixture) are not being considerably modified within the chosen pressure frame. The SC-CO_2 densities and viscosities presented above were computed by the relationship proposed by Pitzer and Schreiber [66], and the empirical equation developed by Altunin and Sakhabetdinov [67], respectively.

On the other hand, the increase of supercritical medium polarity at constant pressure provided an extraction yield up to 1.6 times higher than the operation with pure SC-CO_2. Such evidence has been also reported for other biomass samples, such in an SFE optimization study involving *Eucalyptus globulus* bark [68]. However, the modification of the supercritical CO_2 with ethanol favours majorly the solubilisation of more polar compounds, which may or may not be desirable if the extraction of a specific target molecule/families (such as sterols) is objectively pursued.

Besides the general remark on how ethanol seems to be able to increase η_{Total} , it should be mentioned that different influence grades can be noticed between the values range studied for this factor. Accordingly, the total extraction yield jumps between 0-2.5%wt. EtOH is visibly more modest than those observed between 2.5-5% of ethanol content. Such observation reveals that SFE process is sensitive to the amount co-solvent that is being employed, suffering distinct enhancements depending on the chosen ranges. Such sensitivity should be considered under the light that the amount of hydrophilic extractives are 6.3-10.9 times greater than polar extractives in *E. crassipes* [9]. Hence, the vast amount of polar extractives compared to the lipophilic fraction foster the favourable evolution of η_{Total} with the increase of solvent polarity.

In the whole, the operating conditions that maximize the amount of extractives are 300 bar and 5% ethanol content. These should be compared with the specific performance of sterols uptake, which is objective of the following subsections.

Table 13- Regression coefficients of the full model (FM) obtained for each statistical study; their individual significance at a 95% confidence interval and the respective determination coefficient (bold values represent contributions that are statistically significant).

	Total extraction yield		Total sterol extraction yield		Sterol concentration							
					Total sterol		Stigmasterol		β-Sitosterol		Cholesterol	
	FM	p	FM	p	FM	p	FM	p	FM	p	FM	p
β_0	0.914	**<0.0001**	0.323	**0.0003**	35.258	**0.0005**	24.075	**0.0004**	4.316	**0.0004**	4.762	**0.0008**
β_1	0.0271	0.2170	0.00983	0.3722	0.521	0.695	0.506	0.5581	0.0885	0.542	-0.0803	0.695
β_2	0.225	**0.0010**	0.031	**0.0458**	-3.870	**0.0490**	-2.950	**0.0314**	-0.329	0.0840	-0.444	0.0972
β_3	-0.0307	0.3821	-0.0035	0.8435	0.983	0.6701	0.539	0.7136	0.155	0.537	0.115	0.745
β_4	0.0803	0.0758	-0.034	0.1279	-5.526	0.0774	-3.136	0.1	-0.718	**0.0488**	-1.192	**0.0343**
β_5	0.0231	0.3569	-0.00875	0.5023	-1.299	0.444	-0.401	0.6997	-0.309	0.145	-0.406	0.173
R^2	0.98		0.85		0.860		0.88		0.88		0.88	
R^2_{adj}	0.96		0.60		0.627		0.67		0.68		0.69	

Table 14- Reduced experimental models obtained after discarding the non-significant terms.

Reduced Experimental Models	R^2	Eq.
$\eta_{\text{Total}} = 0.947 + 0.225 \times X_{\text{EtOH}}$	0.92	(18)
$\eta_{\text{TotalSterol}} = 0.298 + 0.031 \times X_{\text{EtOH}}$	0.55	(19)
$C_{\text{TotalSterol}} = 32.230 - 3.870 \times X_{\text{EtOH}}$	0.48	(20)
$C_{\text{Stigm}} = 22.343 - 2.950 \times X_{\text{EtOH}}$	0.61	(21)
$C_{\beta-\text{sitost}} = 4.420 - 0.718 \times X^2_{\text{EtOH}}$	0.42	(22)
$C_{\text{cholest}} = 4.839 - 1.192 \times X^2_{\text{EtOH}}$	0.53	(23)

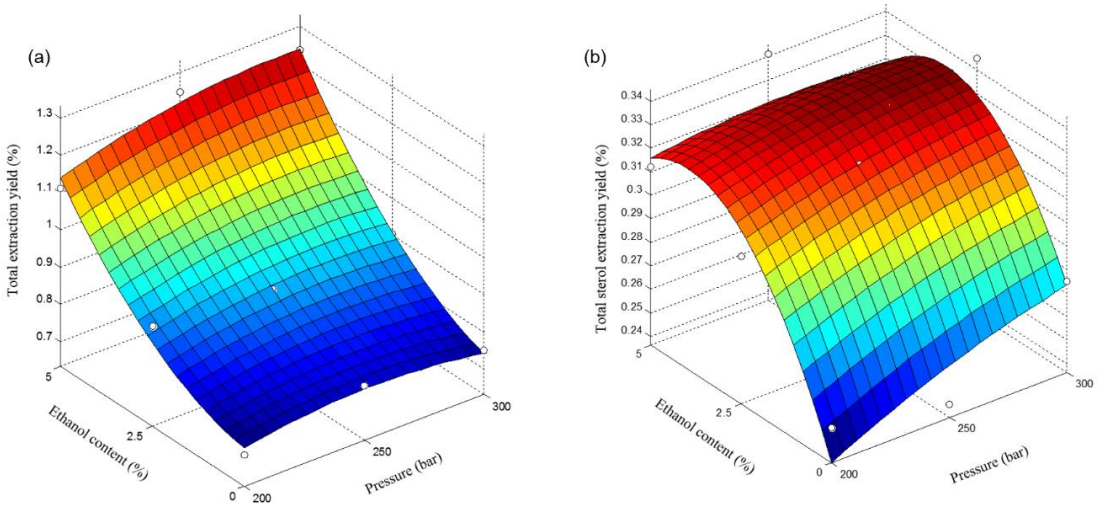

Figure 11 - Response surfaces plotting the effects of pressure and ethanol content over: (a) total extraction yield, and (b) Total sterol extraction yield, for 50 ºC and 7.5 g min^{-1}. Dots are experimental data, and surfaces are given by Table 13.

2.2.3.2.Optimization of total sterols extraction yield ($\eta_{\mathrm{TotalSterol}}$)

Figure 11 (b) presents the extraction profile of sterols as function of ethanol and pressure within the optimized range of values for each factor. Despite of η_{Total} and $\eta_{\mathrm{TotalSterols}}$ visibly follow the same overall trend (i.e. major variations being caused by ethanol content than pressure), the profiles of both yields along the increase of ethanol is distinct for the two responses. In fact, $\eta_{\mathrm{TotalSterols}}$ exhibit a more pronounced increase when moving from 0 to 2.5 wt.% of co-solvent content than η_{Total} response does, but the opposite enhancement is verified within the jump of 2.5 to 5.0% (wt.). This evidence denotes that the uptake of the sterols clearly benefits from a slight tuning of supercritical medium polarity as those implied caused by an addition of 2.5% wt of ethanol, but that above this value no proportional advantage is noticed for $\eta_{\mathrm{TotalSterols}}$. Hence, operation with 5.0% wt. ethanol represents a surplus of co-solvent that has no desirable consequences from a sterols removal point of view.

The advantageous way ethanol can enhance sterols uptake would be undisputable if other compounds were not also present in the biomass samples to be extracted on a competitive basis. In fact, the addition of small quantities of ethanol can boost the molecular interactions between the supercritical solvent and polar compounds, increasing the removal rate of these. As a results significant amount of undesired components may also be recovered, which is not desirable in light of producing extracts with enriched fractions on sterol compounds. As a results, the sterols yield

enhancement through co-solvent addition should be crossed with selectivity criteria, which, in practice, may be analysed finding optimum concentration regions for the sterols**.**

2.2.3.3.Optimization of sterols concentration ($C_{\mathrm{TotalSterol}}, C_{\mathrm{Stigm}}, C_{\beta-\mathrm{sitost}}, C_{\mathrm{cholest}}$)

The last responses evaluated in this work are related to the overall sterols content in the extracts obtained under different operating conditions. Since, as a response, total sterols concentration is built from a ratio between $\eta_{\mathrm{TotalSterol}}$ and η_{Total}, the trends observed for the former two responses may allow anticipating a given concentration profile. In this sense, the acknowledgement that ethanol influences greatly $\eta_{\mathrm{TotalSterol}}$ than η_{Total} with 2.5% (wt.) ethanol, but the opposite is observed with 5.0% (wt.) ethanol, suggests that the region of maximum concentration to be located at the intermediate ethanol content. Figure 12 (a) presents the overall sterols concentration profile along the studied range of operating conditions. As expected, a specific combination of operating conditions contributes to a more selective removal of sterols in contrast to the remaining undesirable compounds available in the biomass, these being 250-300 bar and 2.5% (wt.) ethanol. Overall, the trend observed in the concentration profiles is in agreement with the discussion performed in Section 2.2.3.2, i.e. the conditions that maximizes the sterol concentrations are those where the respective extraction yield achieves its plateau. It is also worth to notice that since a vast amount of hydrophilic compounds are available, the milder ethanol conditions that allow a high removal of sterols are in fact favourable to the goal of having a maximum concentration of these compounds in the extracts.

The existence of a clear optimum region for total sterols concentration in extracts triggered the interest to evaluate also the individual concentrations of the most representative compounds of this family available in the *E. crassipes* extract. Hence, Figure 12 (b), (c) and (d) provide stigmasterol, β-sitosterol and cholesterol concentrations, respectively. These three compounds represent 93-96% of the total sterols concentration of Figure 12 (a). Nevertheless, the individual responses considered gave the same maximum/minimum operating conditions arrangements, these being obtained at Run 8 and Run 9 respectively. As observed in Figure 12 (b), a similarity is noticeable between the concentration profiles of total sterols and stigmasterol. This is due to the fact the latter is the most representative sterol obtained from *E. crassipes*, accounting individually 67-72% of $C_{\mathrm{TotalSterol}}$ in SFE assays, while in Soxhlet it worths 66% of the $C_{\mathrm{TotalSterol}}$ (see Table 11). The very same profile is observed for cholesterol, showing that it shares in great extent with stigmasterol the sensitivity to the pressure and ethanol content conditions, notwithstanding its abundance represents only 11 wt.% of sterols in the studied biomass (see Table 11).

A rather different profile was observed for β-sitosterol (Figure 12 (c)). As a matter of fact, this sterol evidences a greater sensitivity to pressure variations in the range of 200-300 bar than

stigmasterol and cholesterol do. Accordingly, $C_{\beta-\text{sitost}}$ is greatly enhanced by the jump to 300 bar, independently of the ethanol content that is chosen. However, the setting of an intermediate ethanol content (2.5 wt. %) is also preferable as the said enhancement reaches the maximum absolute concentration value on that region.

Taking into account the specificity of β-sitosterol in relation to the other occurring sterols, also that this compound has been reported in several works [22,69,70] as the most abundant sterol present in vegetable biomass (not the case for *E.crassipes*), special attention should be paid when assuming β-sitosterol as representative of the behavior of other existing sterols, whose extraction might be of interest as well.

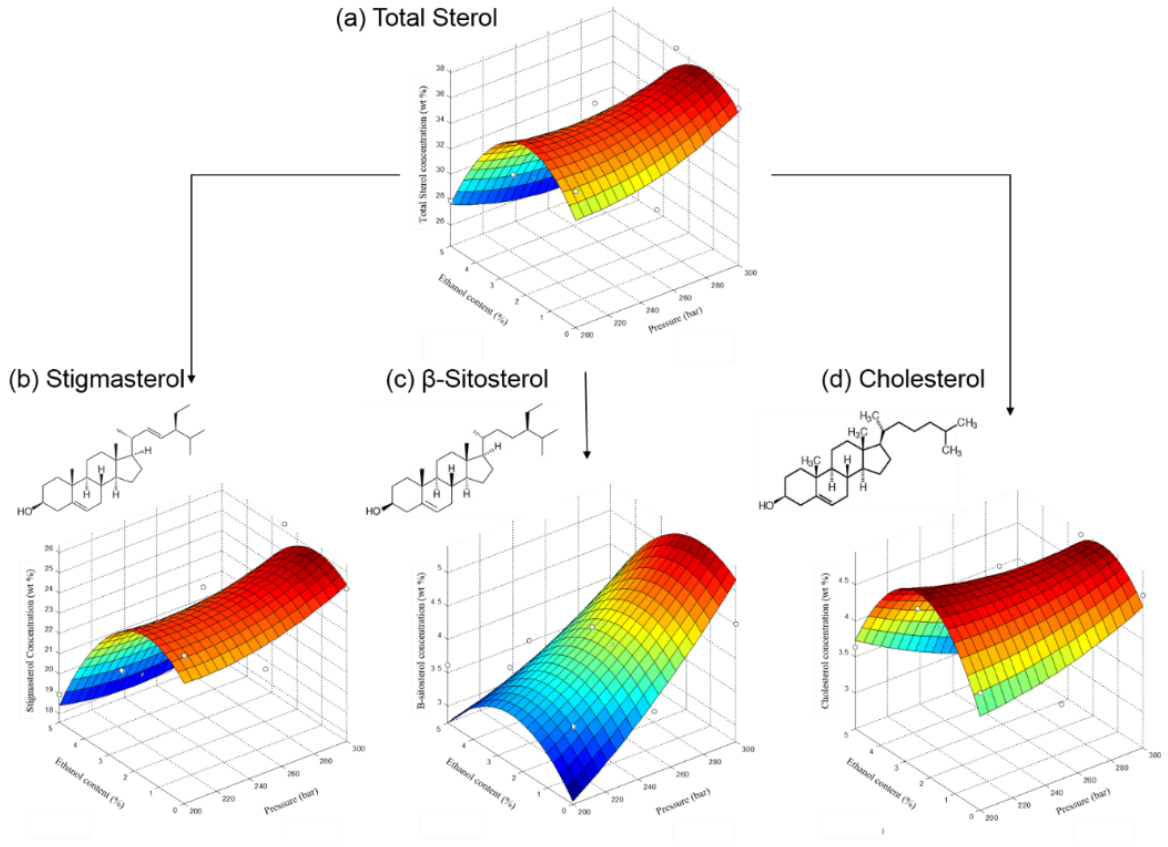

Figure 12 - Response surfaces showing the effects of pressure and ethanol content on the concentration of (a) total sterols, (b) stigmasterol (c) β-sitosterol and (d) cholesterol. Dots are experimental data, and surfaces are given by the fitted full models (Table 13), respectively

2.2.4. Extraction curves measured at optimum conditions

Several extraction curves were measured taking in consideration the trend disclosed by the DoE and optimization study with the aim of unveiling the individual contribution of each factor studied, namely the ethanol contribution and the low influence of pressure in total extraction yield. The aforementioned conditions were those that the extraction yield values attained its minimum and maximum (Run 1 [200bar; 0.0% EtOH] and Run 9 [300 bar; 5.0% EtOH]). For a further comparison, the previously measured extraction curves are also displayed (Run 4 [250 bar; 0.0% EtOH] and Run 6 [250 bar; 5.0% EtOH]) - Figure 13.

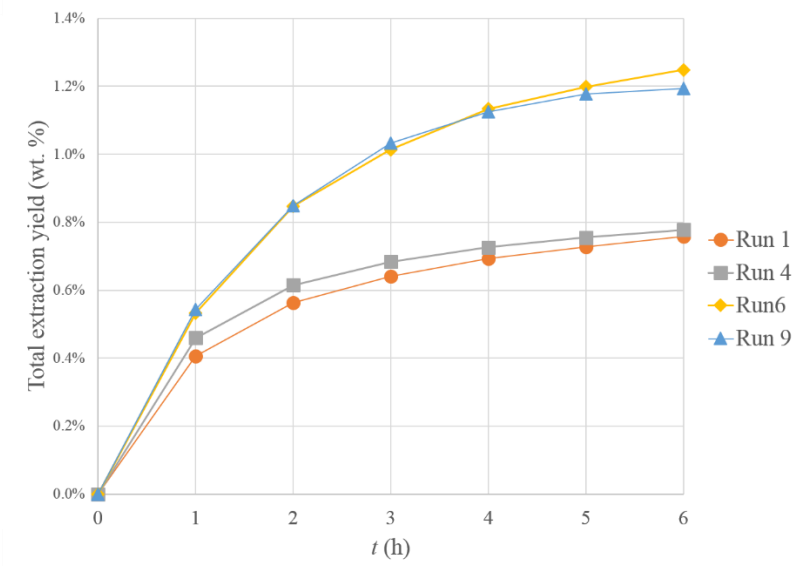

Figure 13- Extraction curves measured around minimum and maximum total extraction yield conditions

From the analysis of the extraction curves, the exact same conclusions obtained from the optimization study can be obtained: at fixed ethanol concentration, the increment of pressure does not affect at all the amount of extract obtained. This fact is observed either at 0.0% EtOH with pressure varying from 200 to 250 bar (where η_{Total} varied 2.63%), and also at 5.0% EtOH for pressure ranging from 250 to 300 bar (with η_{Total} showing fluctuations of 4.33 %). From the overall extraction profile, the overlapping of the extraction curves clearly evidenced the low contribution of pressure in the kinetics of the extraction process.

Regarding the co-solvent contribution towards η_{Total}, an increase of 57 % was obtained when passing from 0 to 5% ethanol concentration in the solvent disregarding the operating pressure, as it was disclosed in the optimization study.

2.2.5. Modeling of the extraction curves

In order to disclose the prevailing transport mechanisms present, several extraction models were tested and the goodness of the fitting was evaluated. The models applied are those identified in the Introduction section (LEFM, SSPM, DFM) and were applied to the extraction curves measured in the experimental assays. The obtained modeling results are displayed in Table 15, including the values of the adjusted parameters, coefficients of adjustment and average absolute relative deviation (AARD). Since the visual shape of the modeled profiles does not vary significantly between experimental curves, Figure 14 provides the graphical representation only for the conditions of minimum and maximum flow rate (i.e. 5.0 g min^{-1} and 10.0 g min^{-1}).

When considering the Linear equilibrium plus Film resistance Model (LEFM) premises, it is important to refer that one of the two parameters, *H*, was fitted simultaneously for the 3 flow rates considered, since the equilibrium conditions do not change when flow rate suffers variations (only the hydrodynamic conditions are affected). Accordingly, the film coefficient was allowed to change for each SFE curve, being noticeable an increment in the $k_f a$ values with the increase of the flow rates. As previously reported (see section 2.2.2), the increment in the film coefficient is more pronounced when passing from 5.0 to 7.5 g min^{-1} (where $k_f a$ increases 1.07 times) than the enhancement from 7.5 to 10.0 g min^{-1} where $k_f a$ increases only by a factor of 1.02, therefore confirming the minimization of the external film layer and making the process mainly controlled by intraparticle diffusion. Regarding the fitting indicators, the coefficient of determination ranges from 87.65 to 94.31% and AARD from 6.39 to 11.44%. It is also important to refer that the poorest fitting is observed for the conditions of highest flow rate, i.e. 10.0 g min^{-1}. Since at this conditions the film resistance is minimized, it is expected that models based in this assumption provides the worst fitting results.

With regard to intraparticle diffusion models, the Simple Single Plate Model (SSPM) and the Diffusion Model (DM) were fitted to the experimental data. Taking into account that a single fitting parameter (the effective diffusivities, D_m/θ^2 or D_m/r^2) was used for the three curves, the results confirmed a good fitting adequacy of these models to the SFE experimental data of *E. crassipes*. In a general view in both models, R^2 ranged from 95.3 to 99.4% and AARD from 3.4 to 10.5%. As a final overall commentary, the modeling performed clearly highlights the major role of intra particle diffusion vs. external mass resistance as the limiting step of the extraction, particularly for flow rates between 7.5 and 10.0 $g_{CO_2}.min^{-1}$.

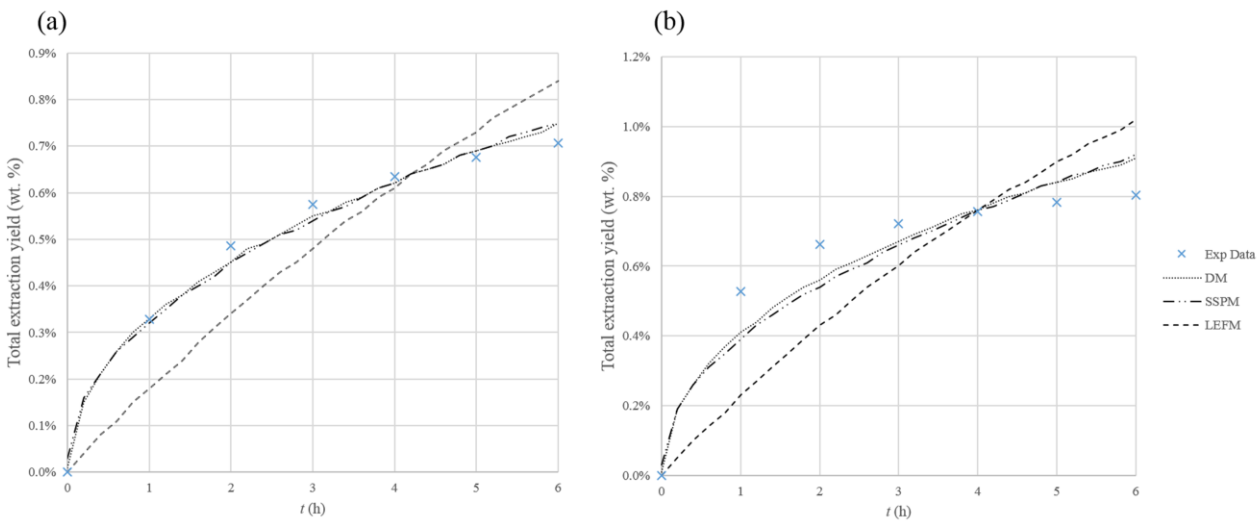

Figure 14 - Fitting of the experimental data to the proposed models – Eq. (9) to (11); Extractions performed at the conditions of 250 bar, 50 ºC, 0% EtOH and (a) 5.0 g_{CO_2} min^{-1} (Run 10); (b) 10.0 g_{CO_2} min^{-1} (Run 11).

Table 15- Optimized parameters and fitting indicators obtained for the extraction models considered for the responses concerning total extraction yield for various flow rates

Exp	$\dot{Q}$ $g_{CO_2}.min^{-1}$	LEFM				SSPM			Diffusion Model		
		H	$k_f a$ $(m \cdot h^{-1})$	R^2	AARD (%)	D_m/θ^2 (h^{-1})	R^2	AARD (%)	D_m/r^2 (h^{-1})	R^2	AARD (%)
Run 10	5.0 g min^{-1}	6.02	0.46	94.31	17.55	0.0063	99.17	9.17	0.0038	99.57	10.29
Run 2	7.5 g min^{-1}		0.49	89.65	20.62		96.83	9.56		97.76	8.25
Run 11	10.0 g min^{-1}		0.50	87.65	21.53		95.26	12.19		96.41	10.29

3. Production of both high quality edible oil and sterols from *Moringa oleifera* seeds: techno-economic optimization of a commercial SFE process

In this section, techno-economic optimization study for the SFE of moringa oil and sterols [15] is presented, where the best operating conditions (pressure, *P*, and extraction time, *t*) to minimize the costs of a manufacturing of an integrated SFE commercial process are targeted.

For this, the hybrid approach comprising response surface methodology and cost of manufacturing (RSM-COM) was employed, requiring the full simulation of the process using Aspen Plus® using SFE experimental data from the literature and the adaption of a patented vacuum distillation process for the separation of the sterols from the vegetal oil, allowing the final delivery of two distinct products.

3.1. Modeling

3.1.1. Solubility estimation

Zhao et al. [11,73] measured the solubility of *Moringa oleifera* oil at 200-500 bar and 60-100ºC. The experimental data obtained was adjusted to the Peng-Robinson equation of state and three density based expressions (Chrastil [47], del Valle and Aguilera [48], and Adachi and Lu [71]). Among these four options, the Chrastil equation modified by del Valle and Aguilera was the one that best fitted the experimental data. Therefore, the estimation of moringa oil solubility in $SC-CO_2$ within the operating conditions studied in this work was accomplished using del Valle and Aguilera modification – Equation (3). The model parameters were adjusted to experimental data and the respective values are $k_1 = 7.22$, $a = -2.3 \times 10^4$ K, $b = 3.31 \times 10^6$ and $c = -8.17$ K^2.

3.1.2. Economic analysis

The analysis using the hybrid RSM-COM approach combines the statistical optimization tool (RSM) with an economic response Cost of Manufacturing (COM), allowing the assessment of the overall impact of the operating conditions in broader extent, as it goes beyond yield and concentration criteria, as it also includes productivity, energy and utilities expenses, among others. As referred previously, the cost of manufacturing (COM) is obtained by Equation (6) and the assumptions required to quantify each parcel individually are presented in Table 16.

The overall integrated process considered for the SFE of *M. oleifera* seeds encompasses a total of three stages: a biomass drying unit, the SFE unit, and a purification unit, with the following features:

(I) The drying unit consists of one belt drying system and is devoted to the reduction of the moisture content from a natural moisture value of 12.34% [72] to 5.88% [13], where steam and electricity are the necessary utilities for this purpose. The predicted investment needed for such solution can be as high as 0.35 M€ [74], which makes drying stage to demand an investment that amounts 11.5% of the one required for the SFE stage.

(II) The SFE unit consists in two extraction vessels of 1 m^3 capacity each (the size was chosen in accordance to the typical availability of the biomass), one CO_2 storage tank, one pump, a heat exchanger, a condenser, a set of valves, and a separator. Being the key stage of the process, the whole unit demands an investment of 3.05M€, which accounts for 88.2% of the investment;

(III) The purification unit consists in a distillation column to be operated under vacuum and sized in accordance with the oil production capacity of the SFE unit (more information is provided in Section 3.1.3.). The investment cost (FCI) for the fractionation column was estimated by the method proposed by Turton et al. [75], which considers the cost of equipment as a function of the operating pressure, materials of construction and geometrical characteristics of the unit. Accordingly, the investment cost for the purification unit amounts only 0.3% of that required for the SFE stage.

Regarding the operation of the SFE unit, a ratio of one employee per extractor was adopted, as well as 24 hours operation per day, during 330 days per year. Furthermore, it was considered that only one extraction cycle takes place at a given time, implying that while one extractor is running the remaining extractor is being prepared. Since two extraction cycles do not occur simultaneously, the extractor in preparation must always wait for the end of the ongoing cycle in order to start. Regarding the separation/collecting vessel, a minimum pressure of 45 bar was admitted, and a temperature of 40 ºC was chosen in accordance to the reference study considered [13]. The costs of utility consumption were obtained from Aspen Plus® v7.3 simulations of the SFE process, as presented in Figure 15.

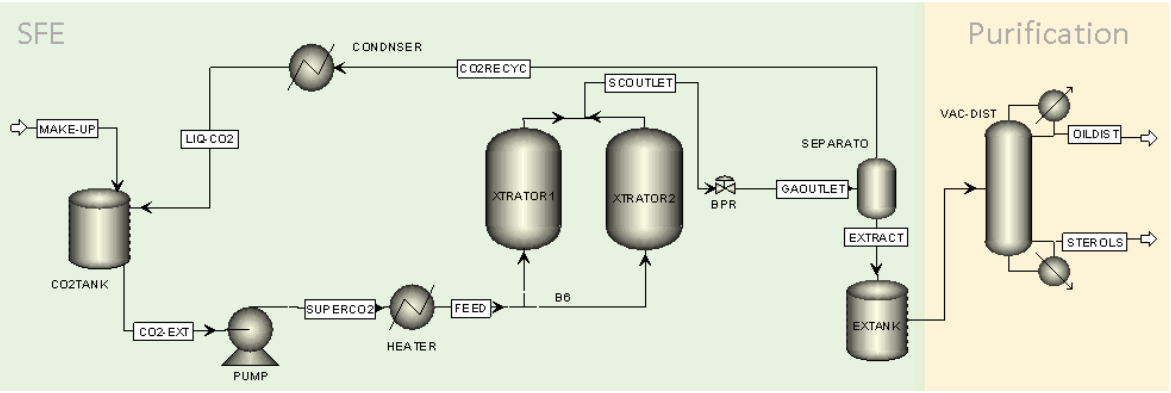

Figure 15 - Process flowsheet used in Aspen Plus® v7.3 for the estimation of the costs related to utilities consumption in the integrated process. The drying stage is not represented.

Beyond COM, the overall net income was also considered for a more complete assessment of the economic performance of the integrated unit, since the revenues of the process may (or may not) compensate higher costs of production and/or oscillations in production volumes. Regarding the pricings of the oil and sterols mixture, conservative values were considered for both products, being these 30 and 350 € kg^{-1}, respectively.

Table 16 - List of assumptions of the economic analysis of the SFE of *Moringa oleifera* oil

General	- Unit working period: 24 h per day, 330 days per year;
	- Number of workers *per* extractor = 1;
	- Scale-up criterion: solvent mass per mass of dried biomass in the extractor $(w_{CO_2}\ w_{biomass}^{-1})$;
	- Extract collection vessel pressure = 45 bar;
	- Extract-collection vessel temperature = 40 ºC
	- Maximum number of extractors in operation: 1 for a scheme of 2 extractors in parallel;
	- Maximum number of extractors under unload/load/repressurization = 1;
	- The fluid losses in each full decompression correspond to the mass of fluid inside the extractor at 45 bar and 40ºC;
	- Bed porosity = 0.8;
	- Exchange ratio $US/€ (on January 2015) = 0.8813;
	- Biomass initial moisture = 12.34% [72];
FCI	- Annual depreciation rate = 10%;
	- Price of a two-extractor of 1 m^3 capacity SFE unit: 3.05 M€;
	- Price of a drying unit: 0.35 M€ [74];
	- Price of distillation column: 55.7 k€
COL	- Labor cost = 10 € $h^{-1}worker^{-1}$;
CUT	- Cost of electricity = 50 € MWh^{-1};
	- Cost of steam = 1.53 € ton^{-1};
	- Drying costs comprise the utilities necessary for the reduction of moringa seed moisture to 5.88% (wt.) [13];
CWT	- Cost of waste treatment = 0 €;
CRM	- Cost of CO_2 = 800 € ton^{-1};

Table 17 - Codifications and levels of correspondence of the variables used in the optimization study.

Factor	Variable	Codified variable	Level of correspondence				
			-1	-0.33	0	0.33	1
pressure (bar)	P	$X_{\mathrm{P}} = (P - 250)/100$	150	-	250	-	350
extraction time (h)	t	$X_{\mathrm{t}} = (t - 2.35)/1.05$	1.3	2.0	-	2.7	3.4

3.1.3. Project and simulation of the purification of sterols in Aspen Plus®

In this work the removal of sterols by high vacuum distillation was adopted following Clark et al. [76] patent, which briefly encompasses a column operating between 240ºC and 196ºC at 0.004 bar. Although high, these temperature values are in the ranges typically employed in post treatment steps of oils such as deodorization [78].

With respect to the feed composition, a representative stream was adopted for the simulations, comprehending the following compounds: oleic acid (85%, w/w), palmitic acid (7.3%), and stearic acid (7.4%) for the fatty acid fraction, and stigmasterol (0.05%) and beta-sitosterol (0.2%) for the sterol fraction of the extract.

The described purification process was adapted to the SFE of ben oil under study, and Aspen plus version 7.3 was used to simulate the distillation columns towards the desired separation. The NRTL model was the thermodynamic expression chosen in the calculations. The first steps of the purification approach comprised the preliminary design of the column for the aforementioned feed composition and operating conditions. The study revealed that a column with 5 theoretical stages, a diameter of 1 meter, a distillation-to-feed ratio of 0.9981, and a reflux ratio five times greater than the minimum (conservative heuristic rule) is able to produce sterols with purity up to 89.4 wt.% (bottom product).

3.2. Results and discussion

3.2.1. Brief description of the extraction curves

The proposed integrated process is based on the experimental SFE data obtained by *Ruttarattanamongkol* et al. [13], namely in the SFE curves measured for conditions of pressure and temperature ranging from 150 to 350 bar and 25 to 35ºC, which are plotted in Figure 16. The supercritical extraction assays were performed in a pilot plant with capacity of 2 L and a load of 850 g of biomass per batch. The system includes an extraction column, a vessel for extract collection (separator), a CO_2 storage tank, a heat exchanger, a piston pump and pressure reduction valve. The CO2 flow rate was maintained at 20 $\mathrm{kg \cdot h^{-1}}$ for each extraction run, and the temperature inside the

separator was fixed at 40 ºC. With regard to sterols quantification, Gas Chromatography-Mass Spectrometry (GC-MS) was employed to assess their concentration in moringa oil samples.

In Table 18 a summary of operating conditions (temperature, flow rate, pressure) of the selected SFE curves is reported, including the estimated oil solubility for the various conditions. In addition, the minimum $\mathrm{COM_{oil}}$ among the extraction times studied is reported, as well as the respective oil production under the conditions of the said minimum $\mathrm{COM_{oil}}$.

In terms of overall trends, Table 18 is quite clear: oil solubility (y^*) increases as pressure is increased, leading to a consequent enhancement in oil production (process productivity) and a decrease in the cost of manufacturing of moringa oil. The course of these trends will be object of statistical confirmation embodied in the RSM-COM analysis.

Table 18 - Compilation of experimental values used in the RSM-COM optimization, minimum $\mathrm{COM_{oil}}$ obtained for each value of P and the respective production and solubility.

T (ºC)	$\dot{Q}$ ($\mathrm{kg_{CO_2}\,h^{-1}}$)	P (bar)	y^* ($\mathrm{g_{oil}\,L_{CO_2}^{-1}}$)	Min $\mathrm{COM_{oil}}$ (€ $\mathrm{kg_{oil}^{-1}}$)	Oil Production @ Min $\mathrm{COM_{oil}}$ ($\mathrm{kg_{oil}\,year^{-1}}$)
30	20	150	1.92	6.52	163 320
		250	3.56	3.81	329 586
		350	5.10	2.64	558 870

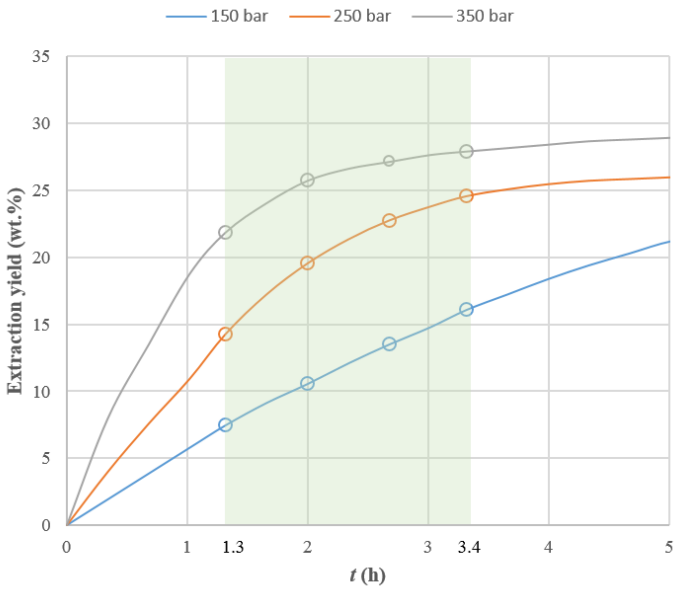

Figure 16 - Experimental extraction yield. Data taken from [13]; the shaded area represents the operating conditions interval where the RSM-COM method was applied

3.2.2. Screening of the significant factors

The RSM-COM approach under discussion is specifically focused on the production of the oil, which means the purification expenses to obtain the sterols fraction were left out of these calculations. In this sense, the bulk oil directly produced by the SFE unit was taken as the product into which $\mathrm{COM_{oil}}$ refers to.

Upon building a regression of $\mathrm{COM_{oil}}$ as function of the process variables, a screening was performed in order not only to evaluate the significance of each effect upon the generic model and to discard the non-significant ones, but also to disclose their impact (positive or negative) on the cost of manufacturing.

In Figure 17 the Pareto diagram concerning the fitted model is presented, being the relative impacts on $\mathrm{COM_{oil}}$ hierarchized from highest contribution (bottom of the graphic) to the lowest contributions (top of the graphic). Observing each variable individually, pressure is clearly the most significant factor, either linearly (P), quadratically (P^2) or crossed with time ($P \times t$). Moreover, this contribution accounts for more than 45% of the weight on the response, being therefore the governing term in the process. While it is known that higher pressures imply greater utilities consumption, the Pareto chart evidences that these expenses do not prevail along pressure increments, since an overall cheapening of the extraction process is reported along P. Remarkably, the linear effect of pressure is the only effect that acts in favor of the economy of the process, i.e. leads to lower $\mathrm{COM_{oil}}$ values. Such behavior has been also reported in the SFE of lycopene [52] and gac oil [74]. The remaining contributions ($t, t^2, P \times t$ and P^2) increase $\mathrm{COM_{oil}}$, being P^2 the second most important effect after P, followed by the crossed contribution between pressure and time ($P \times t$).

The diminution of $\mathrm{COM_{oil}}$ with the increase of pressure can be interpreted in light of y^* dependence commented in Section 3.2.1 and reported in Table 18. The sensitivity of a SFE process to solubility variations becomes more relevant when dealing with biomass of high oil contents (typically the case of the commodity edible oils), since saturation of the supercritical phase is prone to be reached at extractor outlet. Under such circumstances, the oil uptake typically resembles a straight line from the beginning of the SFE onwards, giving rise to the well-known first period of extraction (CER). Since pressure increments increase $\mathrm{SC-CO_2}$ density, which in turn imparts a power law driven increase on the solubility (from Equation (3), $y_\mathrm{i}^* \propto \rho_\mathrm{f}^{k_1}$), the higher the P the more the overall process productivity is increased, which is highly advantageous for SFE economy.

With regard to the effects imparted by extraction time, the strongest influence on $\mathrm{COM_{oil}}$ takes place setting P as moderator ($P \times t$), which means that time affects the results depending on the chosen value of pressure. This result is in agreement with the observations taken from the extraction curves - Figure 16 - in the sense that, while for the curve at 150 bar time seems to be

always advantageous (a linear increase of yield across time), at 250 and 350 bar the extraction rate suffers a progressive decrease along time, making it less worthy to keep the process running from 1.3h to 3.4h. This may be due to the significant enhancement in solubility at higher pressures, which leads to a quicker tendency to remove most of the existing extractives so that providing more time to the process becomes inefficient due to the lack of more extractives to be removed. This is not always observed in the SFE works, as discussed previously, and observed for *E. crassipes* extracts. For instance, for processes where the mass transfer is majorly governed by intraparticle diffusion or external film resistance (through effective diffusivity, D_{eff}, and convective mass transfer coefficient, k_{f}, respectively) the importance of t for the SFE production costs may be much greater, as it has been observed for the SFE of eucalypt bark [68]. On the other hand, when the extraction is essentially governed by solubility, the influence of extraction time on the process is softened and less noticeable, owing to the fact that in such circumstances the SFE process relies mainly on the density of the supercritical solvent, which in turn is a function of pressure and temperature, but not of time.

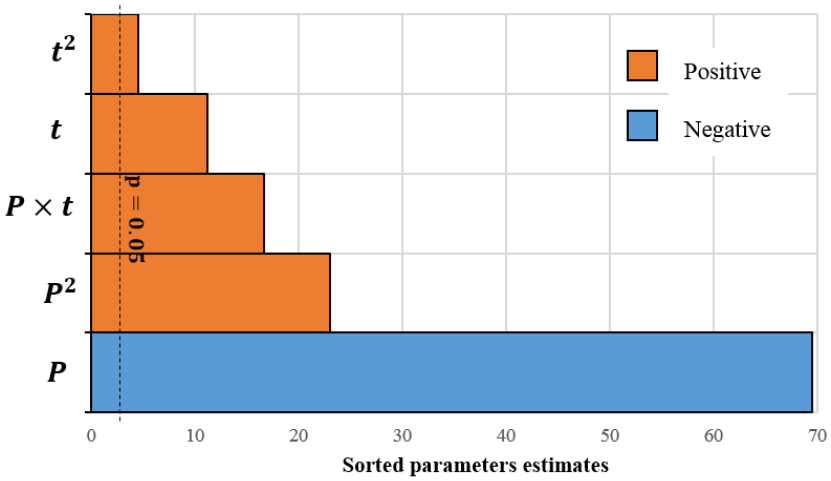

Figure 17 - Statistical analysis of the impact of different factors and interactions upon COM_{oil}. Dashed lines delimit the region of no statistical significance for a 95% confidence interval.

3.2.3. Optimization of the SFE process

Taking into account that all factors (t,t^2,$P \times t$ and P^2) are statistically significant to COM_{oil} for a 95% confidence interval, all of them were maintained in the response surface model. The final uncoded equation is given by:

$$\text{COM}_{\text{oil}} = 9.49 \times 10^{-5} \times P^2 + 5.06 \times 10^{-3} \times P \times t - 7.59 \times 10^{-2} \times P + 0.179 \times t^2 - 1.90 \times t + 17.5 \qquad (24)$$

where $\mathrm{COM_{oil}}$ is expressed in € $\mathrm{kg_{oil}^{-1}}$, P in bar, and t in h, and a coefficient of determination (R^2) of 99.9% was obtained, as well as an AARD of 0.91%. In order to visualize the individual effects imparted by pressure and time, and their conjugated contribution to $\mathrm{COM_{oil}}$, a graphical representation of Equation (24) is plotted in Figure 18. In a first general view, the $\mathrm{COM_{oil}}$ values range from 7.1 € $\mathrm{kg_{oil}^{-1}}$ at 150 bar and 1.3 h, to 2.6 € $\mathrm{kg_{oil}^{-1}}$ at 350 bar and the same extraction time, and at a constant temperature of 30°C.

Within the plotted $[P, t]$ frame of Figure 18, the optima operating conditions are the combination of highest pressure (350 bar) and shortest extraction time (1.3 h). In addition, the fact that the smallest value of t is responsible for both the maximum and minimum $\mathrm{COM_{oil}}$ is an indicator that pressure is in fact the key factor of $\mathrm{COM_{oil}}$.

Since oil solubility increases with increasing pressure, the time required to produce an equal amount of extract (at fixed solvent flow rate) is naturally lower at higher P. Additionally, an operation under quicker extraction cycles allows the number of batches per year to be increased, which enhances the annual oil production. Taking into consideration that $\mathrm{COM_{oil}}$ is indexed to the amount of oil obtained, higher productivity gives rise also to a decrease in the costs of production.

With regard to the market attractiveness of the reported $\mathrm{COM_{oil}}$ values, since moringa oil fatty acid profile is similar to those of high value edible oils (high concentration of oleic and behenic acids) [13], its price can attain values as high as 50 € $\mathrm{kg_{oil}^{-1}}$ [78]. Nonetheless, even adopting a more conservative market price of 30 € $\mathrm{kg_{oil}^{-1}}$ - as it was done for the net income calculations in this work - the proposed process provides competitive results towards the commercialization of this oil.

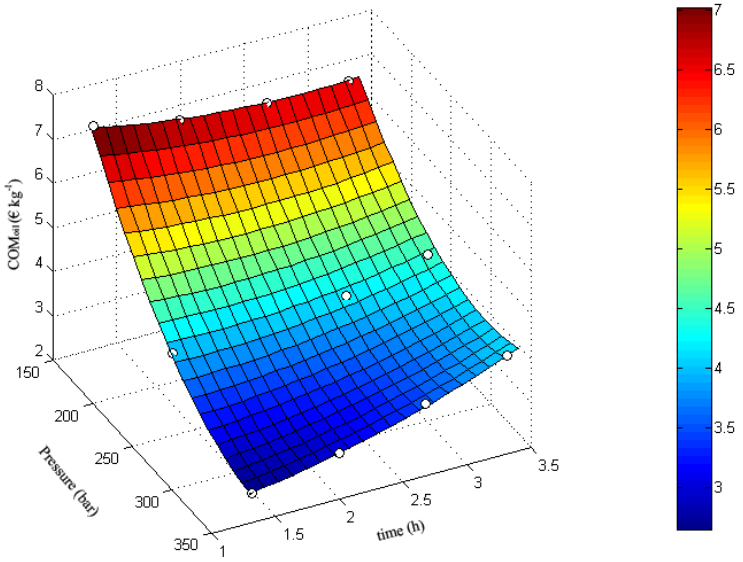

Figure 18 - $\mathrm{COM_{oil}}$ as function of pressure and extraction time. Symbols are calculated results, and the response surface model is Equation (24)

3.2.4. Integrated process with sterol purification

Sterols are a complementary high value fraction of moringa oil that can be exploited as a second independent product of this SFE process, rather than laying as minor components with negligible added value for the bulk oil. Owing to the higher market value of sterols in relation to ben oil, the integration of a sterols purification step after the SFE stage could add more value to the whole process. This was the principle behind studying the inclusion of a purification stage.

As far as the assessment of the process costs for the two products is concerned, they were estimated with the same COM expression used previously (see Equation (24)), but with the following nuances: (i) $\mathrm{COM_{oil}}$ comprises the FCI, CUT, COL costs of the upstream stages of moringa bulk oil production, namely the drying biomass and the supercritical extraction; (ii) $\mathrm{COM_{sterols}}$ comprehends not only the FCI, CUT and COL costs specifically related to the purification goal, but also all the costs implied in the previous production of bulk moringa oil. In practice:

$$\mathrm{COM_{sterols}} = \mathrm{COM_{oil}} + \text{Purification stage costs } (\mathrm{FCI}, \mathrm{CUT}, \mathrm{COL}) \quad (25)$$

While it is clear from the previous topics that the economic attractiveness of sterols isolation depends on the cumulative costs of three stages (drying + SFE + purification), four scenarios involving the operation of the integrated process have been analyzed in this work, by combining different number of workers with distinct production arrangements. In Table 19 the results achieved for the four cases considered are summarized, being the reference scenario a production case where no purification stage exists at all (i.e. only drying + SFE are assumed).

Since the expansion of the process through the introduction of additional units forces the re-arrangement of the work plan of the plant, an additional full-time worker may be necessary to cope with the operation of the distillation column (2nd Scenario). In alternative, one may consider rearranging the production so that the two workers of the reference case can deal both with extraction and purification stages at the expenses of stopping the extraction unit during one day a week, and using that day to purify the oil obtained in the previous six days (3rd Scenario). Finally, the last possibility comprises the ideal situation where the distillation unit can be operated one day a week in parallel to the SFE unit (which in turn operates 7 days per week), with same number of workers of the reference case (4th scenario).

Due to the relatively low amounts of purified sterols obtained from the purification unit (a maximum of 1.9 $\mathrm{ton\ year^{-1}}$), a continuous operation may be not necessary [79]. Hence, a batch or semi-batch distillation was chosen for the sterols isolation, which opened the way for the different scenarios concerning when and how to operate this unit.

Before discussing the performance of $COM_{sterols}$ for each scenario, it is worthwhile to note that COM_{oil} is only affected when less days of production are established for the SFE unit, which happens in the 3rd scenario. In the latter, COM_{oil} jumps to 2.82 € kg_{oil}^{-1} , which represents a cost of production 6.8% greater than the reference value (2.64 € kg_{oil}^{-1}). Furthermore, such constraints on the time devoted to the SFE operation impose a much more significant impact on annual production, which is reduced by 15.8% in the case of the 3rd scenario. This drops the overall net income of the process by 12.8%.

Concerning $COM_{sterols}$, 2nd and 4th scenarios represent opposite realities in terms of human resources synergies for an integrated process like the one considered. In fact, when an extra worker is specifically allocated to the purification process, $COM_{sterols}$ scores 23.12 € $kg_{sterols}^{-1}$. If this extra worker is not hired to cope with the purification stage, $COM_{sterols}$ is decreased by 77.9%, amounting 5.11 € $kg_{sterols}^{-1}$. This clearly underlines the advantages of considering an integrated process (4th scenario) in relation to two independent extraction-purification processes (2nd scenario), answering thus to the opportunity to bridge SFE with post treatment that increase the added-value of the bulk extracts or oils produced.

On the other hand, on a conservative approach it would not be expectable that the same two workers originally devoted to handle the drying and purification units can also cope with the purification stage at the same time, the scenario number 3 overcomes this problem by replacing one day/week of SFE operation by one day/week for purification. Such arrangement allows $COM_{sterols}$ to be decreased 76.5%, to 5.43 € $kg_{sterols}^{-1}$, but a soft penalty of COM_{oil} to 2.82 € kg_{oil}^{-1} is a side consequence. Nonetheless, this option leads to the referred major drawback regarding oil annual production and net income. Hence it can be concluded that it is preferable to operate with a human resources synergy (Scenario 2), than to replace one day of extraction (by purification) in order to avoid expanding the fixed costs through the labor parcel (COL).

Furthermore, an important insight also verified in other RSM-COM work [52] is that the arrangements that minimize the cost of manufacturing may not always be the most favorable conditions to maximize the profits of the process, since the annual net income relies also on the production volumes attained, and also on the market prices of the products in question.

In the whole, the analysis presented in this section shows that the purification approach of the bulk *M. oleifera* oil towards the production of a secondary enriched sterols stream with almost 89.4% purity can be accomplished with advantage as a downstream stage of the SFE unit devoted to the bulk oil production.Due to the fact sterols represent very low fractions of the oil, the economic performance of purification is able to enhance the overall process net income only up to 4.3% (4th scenario). This percentage is fully due to the specific valorization of the 0.25% fraction that sterols represent in the bulk moringa oil, which is a remarkable outcome.

Table 19 - Economic performance of the integrated process (drying + SFE + purification) for several scenarios: assumptions and calculated results.

Scenario	Process workers	SFE	Purification stage	COM (€ kg^{-1})	Production (ton $year^{-1}$)	Net income (M€ $year^{-1}$)
1st case (Reference)	2 (for SFE)	7 days/week	-	Oil = 2.64	Oil = 558.9	15.29
2nd case	2+1 (for SFE + for Purification)	7 days/week	1 day/week	Oil = 2.64 Sterols = 23.12	Oil = 558.9 Sterols = 1.9	15.91
3rd case	2 (for SFE + Purification)	6 days/week	1 day/week	Oil = 2.82 Sterols = 5.43	Oil = 470.8 Sterols = 1.6	13.34
4th case	2 (for SFE + Purification)	7 days/week	1 day/week	Oil = 2.64 Sterols = 5.11	Oil = 558.9 Sterols = 1.9	15.94

4. Conclusions and future work

In this work, supercritical fluid extraction technology was applied and modeled for the production of sterol enriched extracts from both *E. crassipes* and *Moringa oleifera*.

With regard to the SFE of *E. crassipes*, four preliminary extractions curves were measured and suggested that ethanol content should be optimized, and revealed that flow rate should be at least 7.5 g min^{-1}. Based on these insights, statistical optimization (design of experiments, DoE, and response surface methodology, RSM) was performed for pressure (P=200-300 bar) and ethanol content (x_{EtOH} =0-5% wt.). The study covered total extraction yield (η_{Total}), total sterols extraction yield ($\eta_{\mathrm{TotalSterol}}$), and sterols concentration ($C_{\mathrm{TotalSterol}}, C_{\mathrm{Stigm}}, C_{\beta-\mathrm{sitost}}, C_{\mathrm{Cholest}}$). The screening of the factors showed that the contribution x_{EtOH} has a positive synergistic effect in both yield responses. Regarding concentrations, the contrary effect was found. The optimum combination of $[P; x_{\mathrm{EtOH}}]$ are 300 bar and 5.0% (wt.) ethanol for η_{Total}, and 300 bar and 2.5% for $\eta_{\mathrm{TotalSterols}}$, $C_{\mathrm{TotalSterol}}, C_{\mathrm{Stigm}}, C_{\beta-\mathrm{sitost}}$, and C_{Cholest} responses. Finally, 2 additional SFE curves were measured using optimized conditions aiming at studying the kinetics of the process through the application of simplified models based on intraparticle diffusion (DFM and SPPM), and linear equilibrium plus film resistance (LEFM). Accordingly, modeling results confirmed that the external film is minimized at the flow rate of 7.5 g min^{-1} and that the major resistance to mass transfer relies then on intraparticle diffusion. These conclusions were based on the individual fitting indicators: R^2 ranging from 95.26 to 99.57%, and AARD varying from 8.25 to 12.19%.

Regarding *Moringa oleifera*, a techno-economic study was applied to a proposed SFE 1 m^3 extraction capacity industrial plant (including also drying and purification stages) devoted to the production of both edible oil and sterols. RSM was used for the optimization of operating conditions that minimize the cost of manufacturing (COM) of the integrated process. Under optimized conditions of P=350 bar and t=1.3 h, $\mathrm{COM_{oil}}$ =2.64 € $\mathrm{kg_{oil}^{-1}}$ and $\mathrm{COM_{sterols}}$ =5.11 € $\mathrm{kg_{sterols}^{-1}}$ (89.4 wt.% purity). In the whole, a scenario comprising a purification stage operating once a week without the addition of an extra worker leads to an annual productions 558.9 tons of oil and 1.9 tons of sterols with a corresponding estimated positive net income of 15.94M€ $\mathrm{year^{-1}}$.

To conclude, the work provide strong arguments towards the production of sterols (and oil) from vegetable biomass through SFE technology, under the concept of biorefinery.

Future work

The present work provided valuable intel regarding the production of sterols enriched mixtures, either by SFE of *E. crassipes* and M*oringa oleifera*, where the optimization of extraction conditions in the range of 200-300 bar and 0.0-5.0% co-solvent content for the first was assessed, and a techno-economic study and potential implementation of a purification stage was performed for the second.

As an eventual future work, further studies regarding the SFE of *E. crassipes* ought to be performed. More rigorous extraction models should be adjusted to the experimental extraction curves obtained in order to further discuss the rate determining step of the extraction with more detail.

In order to further compare the SFE of *E. crasssipes* and *Moringa oleifera*, an economic analysis of an industrial plant for the production of sterols enriched extracts from *E. crassipes* using RSM-COM could also be a pertinent approach, so that a final techno-economic comparison basis can be reached to support a decision on the most promising way to produce sterols from these vegetable biomass raw materials

5. References

[1] A. Şen, M.M.R. de Melo, A.J.D. Silvestre, H. Pereira, C.M. Silva, Prospective pathway for a green and enhanced friedelin production through supercritical fluid extraction of *Quercus cerris* cork, J. Supercrit. Fluids 97 (2015) 247–255.

[2] J.M. del Valle, Extraction of natural compounds using supercritical CO_2: Going from the laboratory to the industrial application, J. Supercritical Fluids 96 (2014) 180–199.

[3] A. Rahmawati, D. Pang, Y.-H. Ju, F.E. Soetaredjo, O.L. Ki, S. Ismadji, Supercritical CO_2 Extraction of Phytochemical Compounds from *Mimosa pudica Linn*, Chem. Eng. Commun. 202 (2015) 1011–1017.

[4] D.J.S. Patinha, R.M.A. Domingues, J.J. Villaverde, A.M.S. Silva, C.M. Silva, C.S.R. Freire, Lipophilic extractives from the bark of *Eucalyptus grandis x globulus*, a rich source of methyl morolate: Selective extraction with supercritical CO_2, Ind. Crops Prod. 43 (2013) 340–348.

[5] M.M.R. de Melo, a. J.D. Silvestre, C.M. Silva, Supercritical fluid extraction of vegetable matrices: Applications, trends and future perspectives of a convincing green technology, J. Supercrit. Fluids 92 (2014) 115–176.

[6] P. Mäki-Arvela, I. Hachemi, D.Y. Murzin, Comparative study of the extraction methods for recovery of carotenoids from algae: extraction kinetics and effect of different extraction parameters, J. Chem. Technol. Biotechnol. 89 (2014) 1607–1626.

[7] D. Santos, J. Albarelli, M. Rostagno, A. Ensinas, F. Maréchal, M.A. Meireles, New proposal for production of bioactive compounds by supercritical technology integrated to a sugarcane biorefinery, Clean Technol. Environ. Policy. 16 (2014) 1455–1468.

[8] Natex supercritial fluid extraction plants. http://www.natex.at/indusextractionplants.html (accessed May, 2015).

[9] Rui P. Silva, Marcelo M.R. de Melo, Armando J.D. Silvestre, C.M. Silva, Polar and lipophilic extracts characterization of water hyacinth (*Eichhornia crassipes*) roots, stalks, leaves and flowers, and insights for its future valorization, Ind. Crops Prod. (2015).

[10] V.S. J. Tsaknis, S. Lalas, V. Gergis, A total charactherisation of *Moringa oleifera Malawi* seed oil, La Riv. Ital. Delle Sostanze Grasse. LXXV (1998) 21-27.

[11] S. Zhao, D. Zhang, An experimental investigation into the solubility of *Moringa oleifera* oil in supercritical carbon dioxide, J. Food Eng. 138 (2014) 1–10.

[12] S. Mani, S. Jaya, R. Vadivambal, Optimization of Solvent Extraction of Moringa (*Moringa oleifera*) Seed Kernel Oil Using Response Surface Methodology, Food Bioprod. Process. 85 (2007) 328–335.

[13] K. Ruttarattanamongkol, S. Siebenhandl-Ehn, M. Schreiner, A.M. Petrasch, Pilot-scale supercritical carbon dioxide extraction, physico-chemical properties and profile characterization of *Moringa oleifera* seed oil in comparison with conventional extraction methods, Ind. Crops Prod. 58 (2014) 68–77.

[14] R.P.F.F. da Silva, Supercritical fluid extraction of *Eichhornia crassipes*, Master thesis, University of Aveiro, Aveiro, 2014.

[15] P.F. Martins, M.M.R.. de Melo, C.M. Silva, Techno-economic optimization of the subcritical fluid extraction of oil from *Moringa oleifera* seeds and subsequent production of a purified sterols fraction, J. Supercritical Fluids (2015).

[16] P.F. Martins, M.M.R. de Melo, C.M. Silva, P. Sarmento, Supercritical fluid extraction of sterols from *Eichhornia crassipes* biomass using pure and modified carbon dioxide. Enhancement of stigmasterol yield and extract concentration, J. Supercritical Fluids (2015)

[17] S. Rezania, M. Ponraj, M.F.M. Din, A.R. Songip, F.M. Sairan, S. Chelliapan, The diverse applications of water hyacinth with main focus on sustainable energy and production for new era: An overview, Renew. Sustain. Energy Rev. 41 (2015) 943–954.

[18] S. Vidya, L. Girish, Water Hyacinth as a green manure for organic farming, Impact Journals: International Journal of Research in Applied, Natural and Social Sciences, 2 (2014) 65–72.

[19] A. Bhattacharya, P. Kumar, Water hyacinth as a potential biofuel crop, Electron. J. Environ. Agric. Food Chem. 9 (2010) 112-122.

[20] P.S. Pião, L.M.X. Lopes, I.R. Nascimento, Esteróides e um nucleosídeo da macrófita fitorremediadora *Eichhornia crassipes* (Pontederiaceae), 33ª Reunião Anual da Sociedade Brasileira de Química, 2010.

[21] P. Fernandes, J.M.S. Cabral, Phytosterols: applications and recovery methods., Bioresour. Technol. 98 (2007) 2335–50.

[22] C. America, Analytical Characterization of *Moringa oleifera* seed oil Grown in Temperate Regions of Pakistan, 51 (2003) 6558–6563.

[23] S.M. Abdulkarim, K. Long, O.M. Lai, S.K.S. Muhammad, H.M. Ghazali, Some physico-chemical properties of *Moringa oleifera* seed oil extracted using solvent and aqueous enzymatic methods, Food Chem. 93 (2005) 253–263.

[24] Han J.H., Yang Y.X., Feng M.Y., Contents of phytosterols in vegetables and fruits commonly consumed in China, Biomed. Environ. Sci. 21 (2008) 449-453.

[25] Sundararaman P., Djerassi C., A convenient synthesis of progesterone from stigmasterol, J. Org. Chem. 42 (1977) 3633-3634.

[26] S. Panda, M. Jafri, A. Kar, B.K. Meheta, Thyroid inhibitory, antiperoxidative and hypoglycemic effects of stigmasterol isolated from Butea monosperma., Fitoterapia. 80 (2009) 123–6.

[27] T. Woyengo, V. Ramprasath, P. Jones, Anticancer effects of phytosterols., Eur. J. Clin. Nutr. 63 (2009) 813–820.

[28] K. Chung-Oh, Novel stigmasterol derivative or pharmaceutically acceptable salt thereof, method of producing the same, and composition containing the same to inhibit obesity or to prevent and treat hyperlipidemia, WO2008032980 A1, 2008.

[29] T.J. Barder, Purification of sterols with activated carbon as adsorbent and chlorobenze as desorbent, US 4882065, 1989.

[30] P. Alasti, Method for the concentration and separation of sterols, US 6160143, 2000.

[31] Ralph F. Johnson, Jimmy A. De Mars, Process for thermally stabilizing sterols by degassing and flash distilling, US4263103 A, 1981.

[32] M.. Luque de Castro, L.. García-Ayuso, Soxhlet extraction of solid materials: an outdated technique with a promising innovative future, Anal. Chim. Acta. 369 (1998) 1–10.

[33] E. Kiran, M.A.A. Meireles, Workshop on supercritical fluids and energy, Mercado de letras, Campinas, 2013.

[34] P. Sairam, S. Ghosh, S. Jena, K.N. V Rao, D. Banji, Supercritical Fluid Extraction (SFE) - An Overview, Asian Journal of Research in Pharmaceutical Sciences, 2 (2012) 112–120.

[35] J.D. Seader, E.J. Henley, D.K. Roper, Separation Process Principles - Chemical and Biochemical Operations, 3rd ed., John Wiley & Sons, Inc., 2010.

[36] E. Reverchon, I. De Marco, Supercritical fluid extraction and fractionation of natural matter, J. Supercrit. Fluids 38 (2006) 146–166.

[37] G.N. Sapkale, S.M. Patil, U.S. Surwase, P.K. Bhatbhage, Supercritical fluid extraction – A review, ICJS, 8 (2010) 729–743.

[38] K.S. Scott, An evaluation of the use of supercritical fluid extraction techniques to recover drugs from biological matrices, University of Glasgow, 1998.

[39] J.C. Giddings, M.N. Myers, L. McLaren, R.A. Keller, High pressure gas chromatography of nonvolatile species. Compressed gas is used to cause migration of intractable solutes, Science 162 (1968) 67–73.

[40] F. Temelli, O.N. Ciftci, Developing an integrated supercritical fluid biorefinery for the processing of grains, J. Supercrit. Fluids 96 (2014) 77–85.

[41] U. Salgın, A.S. Üstün, Ü. Mehmetoğlu, A. Çalımlı, Supercritical CO_2 extraction of accumulated capsidiol from biotic elicitor-activated *Capsicum annuum L* fruit tissues, J. Chem. Technol. Biotechnol. 80 (2005) 124–132.

[42] H.M. Barbosa, M.M.R. de Melo, M. a. Coimbra, C.P. Passos, C.M. Silva, Optimization of the supercritical fluid coextraction of oil and diterpenes from spent coffee grounds using experimental design and response surface methodology, J. Supercrit. Fluids 85 (2014) 165–172.

[43] S.A.O. Santos, J.J. Villaverde, C.M. Silva, C.P. Neto, A.J.D. Silvestre, Supercritical fluid extraction of phenolic compounds from *Eucalyptus globulus Labill* bark, J. Supercrit. Fluids 71 (2012) 71–79.

[44] G. Vasapollo, L. Longo, L. Rescio, L. Ciurlia, Innovative supercritical CO_2 extraction of lycopene from tomato in the presence of vegetable oil as co-solvent, J. Supercrit. Fluids 29 (2004) 87–96.

[45] B. Palenzuela, L. Arce, a. MacHo, E. Muñoz, a. Ríos, M. Valcárcel, Bioguided extraction of polyphenols from grape marc by using an alternative supercritical-fluid extraction method based on a liquid solvent trap, Anal. Bioanal. Chem. 378 (2004) 2021–2027.

[46] S.G. Ozkal, Supercritical carbon dioxide extraction of apricot kernel oil, PhD thesis, School of Natural and Applied Sciences of the Middle East Technical University, 2004.

[47] J. Chrastil, Solubility of solids and liquids in supercritical gases, J. Phys. Chem. 86 (1982) 3016–3021.

[48] J.M. Del Valle, J.M. Aguilera, An improved equation for predicting the solubility of vegetable oils in supercritical carbon dioxide, Ind. Eng. Chem. Res. 27 (1988) 1551–1553.

[49] C.C.W. Guthrie, NIST/SEMATECH e-Handbook of Statistical Methods, (2013). http://www.itl.nist.gov/div898/handbook/ (accessed May 20, 2015).

[50] R. Turton, R.C. Bailie, W.B. Whiting, J.A. Shaeiwitz, Analysis, Synthesis and Design of Chemical Processes, 2nd ed., Prentice Hall, 2003.

[51] M.M.R. de Melo, H.M. Barbosa, C.P. Passos, C.M. Silva, Supercritical fluid extraction of spent coffee grounds: Measurement of extraction curves, oil characterization and economic analysis, J. Supercrit. Fluids 86 (2014) 150–159.

[52] A.F. Silva, M.M.R. de Melo, C.M. Silva, Supercritical solvent selection (CO_2 versus ethane) and optimization of operating conditions of the extraction of lycopene from tomato residues: Innovative analysis of extraction curves by a response surface methodology and cost of manufacturing hybrid ap, J. Supercrit. Fluids, 95 (2014) 618-627.

[53] M. Perrut, Supercritical Fluid Applications: Industrial Developments and Economic Issues, Ind. Eng. Chem. Res. 39 (2000) 4531–4535.

[54] J.M. Prado, I. Dalmolin, N.D.D. Carareto, R.C. Basso, A.J.A. Meirelles, J. Vladimir Oliveira, Supercritical fluid extraction of grape seed: Process scale-up, extract chemical composition and economic evaluation, J. Food Eng. 109 (2012) 249–257.

[55] R.K. Sinnott, Coulson & Richardon's Chemical Engineering Design, 4th ed., Butterworth-Heinemann, 2005.

[56] L.M.A.S. Campos, E.M.Z. Michielin, L. Danielski, S.R.S. Ferreira, Experimental data and modeling the supercritical fluid extraction of marigold (*Calendula officinalis*) oleoresin, J. Supercrit. Fluids 34 (2005) 163–170.

[57] M.M.R. de Melo, R.M.A. Domingues, M. Sova, E. Lack, H. Seidlitz, F. Lang Jr., Scale-up studies of the supercritical fluid extraction of triterpenic acids from *Eucalyptus globulus* bark, J. Supercrit. Fluids 95 (2014) 44–50.

[58] C.S.G. Kitzberger, R.H. Lomonaco, E.M.Z. Michielin, L. Danielski, J. Correia, S.R.S. Ferreira, Supercritical fluid extraction of *shiitake* oil: Curve modeling and extract composition, J. Food Eng. 90 (2009) 35–43.

[59] N. Mezzomo, J. Martínez, S.R.S. Ferreira, Supercritical fluid extraction of peach (*Prunus persica*) almond oil: Kinetics, mathematical modeling and scale-up, J. Supercrit. Fluids 51 (2009) 10–16.

[60] F. Gaspar, T. Lu, R. Santos, B. Al-Duri, Modelling the extraction of essential oils with compressed carbon dioxide, J. Supercrit. Fluids 25 (2003) 247–260.

[61] J. Crank, The Mathematics of Diffusion, Second, Claredon Press, Oxford, 1975.

[62] M.. Cocero, J. García, Mathematical model of supercritical extraction applied to oil seed extraction by CO_2+saturated alcohol — I. Desorption model, J. Supercrit. Fluids 20 (2001) 229–243.

[63] W.E. Schiesser, The Numerical Method of Lines: Integration of Partial Differential Equations, Academic Press, 1991.

[64] R.M. Domingues, E.L.G. Oliveira, C.S.R. Freire, R.M. Couto, P.C. Simões, C.P. Neto, Supercritical Fluid Extraction of *Eucalyptus globulus* Bark-A Promising Approach for Triterpenoid Production., Int. J. Mol. Sci. 13 (2012) 7648–62.

[65] E.L.G. Oliveira, A.J.D. Silvestre, C.M. Silva, Review of kinetic models for supercritical fluid extraction, Chem. Eng. Res. Des. 89 (2011) 1104–1117.

[66] K.S. Pitzer, D.R. Schreiber, Improving equation-of-state accuracy in the critical region; equations for carbon dioxide and neopentane as examples, Fluid Phase Equilib. 41 (1988) 1–17.

[67] M.S. V.V. Altunin, Viscosity of Liquid and Gaseous Carbon- Dioxide at Temperatures of 220-1300 K and Pressures up to 1200 Bar, Therm. Eng. 19 (1972) 124–129.

[68] R.M.A. Domingues, M.M.R. de Melo, E.L.G. Oliveira, C.P. Neto, A.J.D. Silvestre, C.M. Silva, Optimization of the supercritical fluid extraction of triterpenic acids *from Eucalyptus globulus* bark using experimental design, J. Supercrit. Fluids 74 (2013) 105–114.

[69] E.H.K. Sin, R. Marriott, A.J. Hunt, J.H. Clark, Identification, quantification and Chrastil modelling of wheat straw wax extraction using supercritical carbon dioxide, Comptes Rendus Chim. 17 (2014) 293–300.

[70] M.S. Ekinci, M. Gürü, Extraction of oil and β-sitosterol from peach (*Prunus persica*) seeds using supercritical carbon dioxide, J. Supercrit. Fluids 92 (2014) 319–323.

[71] B.C.-Y.L. Y. Adachi, Supercritical fluid extraction with carbon dioxide and ethylene, Fluid Phase Equilib. 14. (1983) 147-156.

[72] Cambodia Tree Seed Project; Seed Testing Reports: *Moringa oleifera*

[73] S. Zhao, D. Zhang, Supercritical fluid extraction and characterisation of *Moringa oleifera* leaves oil, Sep. Purif. Technol. 118 (2013) 497–502.

[74] P.F. Martins, M.M.R. de Melo, C.M. Silva, Gac oil and carotenes production using supercritical CO_2: Sensitivity analysis and process optimization through a RSM–COM hybrid approach, J. Supercrit. Fluids 100 (2015) 97–104.

[75] R. Turton, R.C. Bailie, W.B. Whiting, J.A. Shaeiwitz, D. Bhattacharyya, Cost Equations and Curves for the CAPCOST Program, in: Anal. Synth. Des. Chem. Process., 4th ed., Prentice Hall, Ann Arbo, 2012.

[76] J.P. Clark, A.D. Jimmy, G.G. Wilson, Purification of sterols by distillation, US 3879431 A, 1975.

[77] F.A. Dudrow, Deodorization of edible oil, J. Am. Oil Chem. Soc. 60 (1983) 272–274.

[78] Lala Essential Oil, Moringa Oil - Carrier Oils. http://www.lalaessentialoils.com/moringa-oil.html (accessed March 1, 2015).

[79] J.M. Douglas, Conceptual Design of Chemical Processes, Internatio, McGraw-Hill, Singapore, 1988.

6. Appendix

In this section, additional experimental data gathered throughout this work is displayed, namely the data points of the extraction curves measured at different conditions and the respective responses.

Table A.1 - Experimental points of the cumulative SFE curves of *E. crassipes*

P (bar)	T (ºC)	%EtOH	$\dot{Q}$ ($g \cdot min^{-1}$)	Response (yield wt.%)	*t* (h)						
					0	1	2	3	4	5	6
250	50	0	5	Total	0.00	0.329	0.486	0.575	0.635	0.676	0.706
				Cholesterol	0.00	0.012	0.018	0.021	0.022	0.024	0.024
				Methylcholesterol	-	-	-	-	-	-	-
				Stigmasterol	0.00	0.075	0.118	0.139	0.152	0.161	0.167
				β-sitosterol	0.00	0.012	0.019	0.022	0.024	0.025	0.026
250	50	0	7.5	Total	0.00	0.460	0.615	0.683	0.726	0.755	0.778
				Cholesterol	0.00	0.016	0.022	0.025	0.026	0.027	0.028
				Methylcholesterol	0.00	0.009	0.012	0.014	0.014	0.015	0.015
				Stigmasterol	0.00	0.106	0.143	0.160	0.167	0.172	0.176
				β-sitosterol	0.00	0.017	0.023	0.025	0.027	0.028	0.029
250	50	0	10	Total	0.00	0.527	0.661	0.721	0.756	0.783	0.803
				Cholesterol	0.00	0.021	0.025	0.026	0.027	0.027	0.028
				Methylcholesterol	0.00	0.012	0.014	0.015	0.016	0.016	0.016
				Stigmasterol	0.00	0.125	0.151	0.160	0.166	0.170	0.173
				β-sitosterol	0.00	0.020	0.024	0.026	0.027	0.028	0.028
250	50	5	7.5	Total	0.00	0.533	0.847	1.013	1.133	1.198	1.248
				Cholesterol	0.00	0.027	0.037	0.040	0.042	0.043	0.043
				Methylcholesterol	0.00	0.014	0.019	0.021	0.022	0.022	0.022
				Stigmasterol	0.00	0.142	0.194	0.212	0.224	0.228	0.231
				β-sitosterol	0.00	0.025	0.036	0.040	0.042	0.043	0.044
200	50	0	7.5	Total	0.00	0.405	0.562	0.641	0.694	0.728	0.758
				Cholesterol	0.00	0.018	0.027	0.031	0.033	0.035	0.036
				Methylcholesterol	0.00	0.009	0.014	0.016	0.017	0.018	0.018
				Stigmasterol	0.00	0.128	0.174	0.198	0.218	0.220	0.229
				β-sitosterol	0.00	0.019	0.027	0.031	0.033	0.034	0.036
300	50	5	7.5	Total	0.00	0.544	0.849	1.033	1.125	1.177	1.194
				Cholesterol	0.00	0.025	0.034	0.039	0.042	0.043	0.044
				Methylcholesterol	-	-	-	-	-	-	-
				Stigmasterol	0.00	0.128	0.174	0.198	0.218	0.226	0.229
				β-sitosterol	0.00	0.028	0.036	0.041	0.045	0.047	0.047